NASA CR 137,795

ADVANCED RECORDING AND PREPROCESSING OF PHYSIOLOGICAL SIGNALS

By P. B. Bentley

November 1975

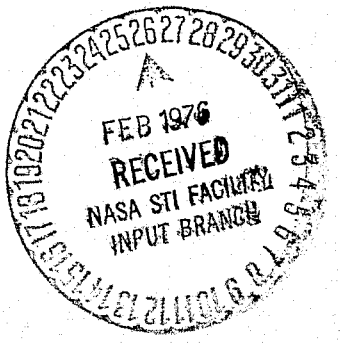

Prepared under Contract No. NAS2-8836 by
STANFORD RESEARCH INSTITUTE
Menlo Park, California

for

AMES RESEARCH CENTER
NATIONAL AERONAUTICS AND SPACE ADMINISTRATION

SECURITY CLASSIFICATION OF THIS PAGE (When Data Entered)

REPORT DOCUMENTATION PAGE

READ INSTRUCTIONS BEFORE COMPLETING FORM

1. REPORT NUMBER

2. GOVT ACCESSION NO.

3. RECIPIENT'S CATALOG NUMBER

4. TITLE (and Subtitle)

ADVANCED RECORDING AND PREPROCESSING OF PHYSIOLOGICAL SIGNALS

5. TYPE OF REPORT & PERIOD COVERED

Final Report
Covering the period May through October 1975

6. PERFORMING ORG. REPORT NUMBER

SRI Project 4260

7. AUTHOR(s)

Philip B. Bentley

8. CONTRACT OR GRANT NUMBER(s)

Contract NAS2-8836

9. PERFORMING ORGANIZATION NAME AND ADDRESS

Stanford Research Institute
333 Ravenswood Avenue
Menlo Park, California 94025

10. PROGRAM ELEMENT, PROJECT, TASK AREA & WORK UNIT NUMBERS

11. CONTROLLING OFFICE NAME AND ADDRESS

National Aeronautics and Space Administration
Ames Research Center
Moffett Field, California 94035

12. REPORT DATE

November 1975

13. NO. OF PAGES

89

14. MONITORING AGENCY NAME & ADDRESS (if diff. from Controlling Office)

15. SECURITY CLASS. (of this report)

Unclassified

15a. DECLASSIFICATION/DOWNGRADING SCHEDULE

N/A

16. DISTRIBUTION STATEMENT (of this report)

17. DISTRIBUTION STATEMENT (of the abstract entered in Block 20, if different from report)

18. SUPPLEMENTARY NOTES

19. KEY WORDS (Continue on reverse side if necessary and identify by block number)

Physiological signals
Blood flow
Ultrasonics
Transcutaneous measurement
Digital recording
Computer processing
Flowmeter evaluation

20. ABSTRACT (Continue on reverse side if necessary and identify by block number)

The measurement of the volume flow-rate of blood in an artery or vein requires both an estimate of the flow velocity and its spatial distribution and the corresponding cross-sectional area. Transcutaneous measurements of these parameters can be performed using ultrasonic techniques that are analogous to the measurement of moving objects by use of a radar. Much of the technology from the field

DD FORM 1 JAN 73 1473

EDITION OF 1 NOV 65 IS OBSOLETE

SECURITY CLASSIFICATION OF THIS PAGE (When Data Entered)

19. KEY WORDS (Continued)

20 ABSTRACT (Continued)

of radar can be applied to the blood-flow measurement task, especially the considerable knowledge about data handling, processing, and displaying.

This report presents the work performed by Stanford Research Institute for NASA-Ames to apply modern digital data recording and preprocessing methods to the measurement of blood-flow velocity by means of the CW Doppler ultrasonic technique. Here only the average flow velocity is measured and no distribution or size information is obtained. The work included evaluations of current flowmeter design and performance, ultrasonic transducer fabrication methods, and other related items. The main thrust of the work was the development of effective data-handling and processing methods by application of modern digital techniques.

The evaluation portion resulted in useful improvements in both the flowmeter instrumentation and the ultrasonic transducers. The analysis work developed effective digital processing algorithms that provided enhanced blood-flow measurement accuracy and sensitivity. The overall result of the contract work has contributed to the utility of the CW ultrasonic Doppler flowmeter as employed by NASA-Ames in their bioengineering research.

CONTENTS

ILLUSTRATIONS

TABLES

I SUMMARY

This report discusses the work performed by the Stanford Research Institute during the period from 1 May 1975 through 15 October 1975 on the application of modern radar data-processing techniques to the extraction of blood-flow parameters using ultrasonic CW Doppler measurement methods. Both general and specific problems relating to the work being performed by the NASA-Ames Research Center at Moffett Field, California have been studied, with results and recommendations transmitted orally to the contract technical monitor. About half of the research effort was directed toward enhancing the performance of specific instrumentation used in the ultrasonic blood-flow measurements. A second major part of the effort has been the pursuit of effective digital-processing algorithms to increase the accuracy, resolution, and sensitivity of the analog instrumentation. A small effort was also undertaken to survey the state of the art in ultrasonic transducer performance and fabrication techniques in hopes of improving specific aspects of measuring transcutaneous, noninvasive blood flow.

The evaluation of the blood flowmeter manufactured by L&M Electronics Inc. resulted in the suggestion of several modifications. These were incorporated into the equipment and were found to improve device sensitivity and eliminate anomalous behavior. It is now believed that this equipment is nearly optimum and can be considered a prototype base-line model for the CW Doppler blood-flow technique.

The transducers used with the L&M flowmeter were evaluated by comparative testing in terms of energy-conversion efficiency, element amplitude response matching, and fabrication quality control. An information

interchange among NASA-Ames, L&M, and SRI during this work proved helpful in the development and construction of new and better transducer arrays for enhanced and more reliable performance. An attempt was made to produce an improved transducer that showed comparable efficiency while providing substantially greater useful frequency bandwidth.

The application of modern digital data-processing methods to the Doppler blood-flow measurement was successful. This portion of the work consisted in digitization of the analog output signals from the L&M flowmeter, format conversion, and storage on digital magnetic tapes. These tapes then were used to input the data to a large, general-purpose scientific computer facility for the actual processing. This involved the development of appropriate Fourier transforms, first-moment frequency algorithms, smoothing functions, and output display routines. A variety of data were processed including analog tape-recorded signals taken during acceleration stress testing of human subjects on the NASA-Ames centrifuge and nonstress testing of volunteer subjects at SRI, Menlo Park. The effectiveness of the digital processing was evaluated by comparing it to the effectiveness of the flowmeter analog processing in terms of time-dynamics fidelity, noise, artifact immunity, and sensitivity. Digital processing was found to be equal, if not superior, to analog processing and indicates potentially more accuracy and sensitivity.

II INTRODUCTION

The measurement of blood-flow velocity by use of the ultrasonic Doppler method is fairly well developed, and several successful instruments are being used in both research and clinical applications. However, there are still problems and limitations to overcome. In the work reported here, we have applied new ideas toward improving the accuracy, sensitivity, and reliability of flow-metering techniques.

The main thrust of this work was the application of modern digital data-processing methods to the extraction of pulsatile blood-flow velocity from an artery or vein by use of transcutaneous ultrasonic CW Doppler techniques. The signals that are generated by the flowmeter equipment are complex, noise-like waveforms. Theoretical treatment has shown that a particular mathematical relationship exists between this signal and the mean pulsatile blood-flow velocity in the subject vessel. It is this mathematical relationship that must be used in the signal-conversion process, and digital methods are very effective in the implementation.

The current method of estimating the pulsatile flow velocity is the so-called zero-crossing counter (ZCC). This simple and elegant analog circuitry effectively processes the complex Doppler waveforms and provides a useful but unfortunately incorrect estimate of the flow velocity. However, since the error is not excessive, in many applications the performance is adequate. Therefore, for purposes of evaluation, the results from the digital processing can be compared against the ZCC, especially in terms of ultimate sensitivity and the time dynamics. Accuracy can be assessed only under controlled and calibrated test conditions where the flow is measured by independent and accurate means.

In this work we have attempted to evaluate individual elements of the transducer instead of evaluating the performance of the total array. How well the array may work depends of course on its geometry, but if the basic elements are poorly designed, incorrectly built, misinstalled in the array, then overall performance will suffer. The particular items of interest are (1) basic element energy-conversion efficiency, which affects measurement sensitivity, (2) element amplitude-vs-frequency response in terms of bandwidth, which relates to array versatility, (3) element-fabrication quality control, which determines array element matching for optimum sensitivity, and (4) assembly mounting techniques, which also determine array performance.

Often equipment that is developed for a new measurement technique evolves to a state of semiperfection only after a long period of trial-and-error testing and modification. At some point in the development it may be appropriate to reassess the overall concept in terms of system requirements to determine whether a redirection and reconfiguration is needed, or whether only minor modifications are needed to bring the product up to optimum status. We have used this philosophy in the evaluation of the L&M flowmeter by applying analysis methods that have been used in the field of radio and radar systems for many years. The basic concept is that of signal conditioning to minimize equipment noise and to optimize gain, bandwidth, and dynamic range throughout the equipment.

III BACKGROUND

Physiological researchers have used ultrasonic energy for about 15 years to determine instantaneous velocity and flow information within intact blood vessels. Results obtained from such measurements have provided increasingly valuable insight into hemodynamic functions and characteristics of the cardiovascular and circulatory systems. Additionally, blood-flow information provided by ultrasonic measuring devices has been used recently as a noninvasive indicator of the limitations of humans subjected to stresses that are in extreme contrast to the normal hemostatic environment. Research is currently under way to establish standards and develop instrumentation that would allow accurate quantitative prediction of the conditions that lead to loss of voluntary perceptual control. Given this prediction capability, steps could possibly be taken to counteract the effects of these conditions as they approached maximum human endurance levels. This type of information would be especially valuable in manned space exploration and also in supersonic flight situations in which human controllers are subjected to elevated gravitational forces that have been known to produce loss of consciousness over extended periods of time.

Current ultrasonic-flow detection devices make use of the Doppler effect in which the flow velocity is proportional to the apparent shift in frequency. A block diagram of a representative continuous-wave (CW) system use for obtaining transcutaneous Doppler flow information is shown in Figure 1. A continuous beam of 3-to-10-MHz ultrasound is transmitted via a piezoelectric transducer diagonally through the skin into the blood vessel. Ultrasound scattered by moving red blood cells excites the receiving transducer. The received signal consists of a large-amplitude,

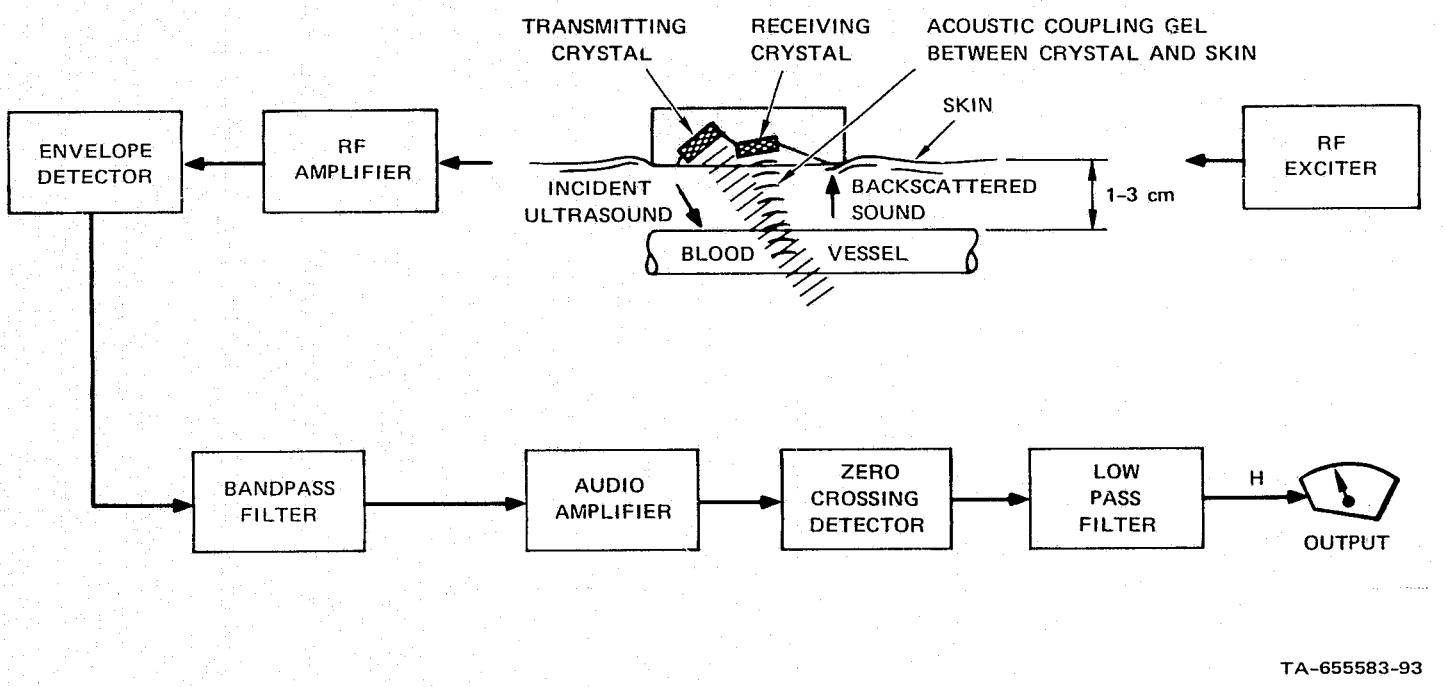

FIGURE 1 BLOCK DIAGRAM OF THE NONDIRECTIONAL DOPPLER ULTRASONIC BLOOD FLOWMETER

excitation-frequency component directly coupled from transmitter to receiver, plus the small-amplitude, Doppler-shifted components backscattered from the blood cells and other tissue that may be moving.

These Doppler components encompass a range of audio frequencies that modulate the ultrasonic excitation carrier frequency. In the return signal, these audio frequencies are in two bands on either side of the carrier frequency, with the upper sideband corresponding to blood flow toward the transducers and the lower sideband corresponding to flow away from the transducer. Most current systems use an envelope type of detector that extracts audio frequencies by essentially removing the carrier so that the Doppler-frequency band starts at zero frequency and contains both the upper- and the lower-sideband energy corresponding to the blood movement in either direction--i.e., the direction of flow is not distinguishable. The output of the detector is then applied to a zero-crossing counter (ZCC) that has an output proportional to the Doppler frequency shift and hence to the blood-flow velocity.

Measurement of the Doppler-frequency shifts in intact blood vessels is complicated for several reasons:

- The Doppler signal is composed of many frequencies, which reflects the fact that the blood flow is not uniform across the vessel. This spread in the signal spectrum means that some averaging method must be used to estimate the true average flow velocity. The output of the ZCC is known to introduce errors because of the manner in which it processes the flow signals. Also, the simple envelope-detection scheme does not recognize flow direction. Newer implementations have corrected that deficiency, but the ZCC-caused errors still remain.
- The desired return signal is often on the order of 90 dB below the carrier because of signal leakage between transmit and receive transducers, attenuation of the backscattered Doppler signal through skin and tissue, and the presence of stationary reflecting elements in the vicinity of the vessel being monitored (bones, muscle, and so on).

- Low-frequency, high-amplitude vessel wall motion can also cause errors in the results obtained with the ZCC. Current bandpass filtering schemes attempt to mask out these effects, but any Doppler information contained below the cutoff point of the filter is lost for analytic purposes. The need for more investigation in this area is obvious.

Direct-frequency analysis of the Doppler spectrum can provide a method to alleviate the problems of using the ZCC. It can also allow inspection of the details of the Doppler spectrum, which could add insight into the proper selection of frequency-filtering boundaries and characteristics. Real-time signal-processing and statistical estimation and pattern-recognition techniques may elicit additional information concerning hemodynamic responses under normal and average stress conditions. Also, different methods of displaying the spectrum could possibly enhance the quality and quantity of useful information obtained.

Most currently available spectrum analyzers are limited to about 60 dB in dynamic range and about 10 kHz in bandwidth, which unfortunately are significantly below the 90-dB and 15-kHz values cited above. The problem becomes even more complicated when real-time processing is desired. Using the fast Fourier transform (FFT) to obtain the Doppler spectrum provides additional speed and resolution potential, but often requires complex and expensive equipment to obtain the desired results. Also, the amount of programming necessary to perform the FFT with conventional algorithms usually requires significant digital computer time and capacity. Thus, although FFT processing can contribute greatly to flow-measuring systems, the cost incurred in implementing such systems with commercially available equipment usually prohibits their use by physiological researchers.

IV ANALYSIS OF TECHNIQUES

As mentioned before, the measurement of blood flow by ultrasonic Doppler methods has been performed for many years. Only recently, however, have there been comprehensive investigations into the theory behind the technique, and the application of those discoveries to the instrumentation. For certain uses the blood-flow measurement need be only that of the average velocity, while for others a more detailed flow-velocity-profile estimate is needed so as to permit estimation of actual volume flow rate. In all cases it is advantageous, if not necessary to make these measurements without actually opening the vessel and, if at all possible, without any invasion of the body. Ultrasonic techniques can provide this capability, but the step from velocity measurements to volume flow estimation is large and involves considerable complexity.

Average flow velocity can be easily measured by the use of the transcutaneous CW Doppler flowmeter, but accuracy is still a problem. W. R. Brody presented a fairly comprehensive analysis of the ultrasonic blood flowmeter technique in which he calculated theoretical Doppler spectra as a function of vessel illumination geometry.[1]* He also developed useful mathematical relationships for the flow-velocity estimation from the Doppler signals and the variance of those estimates. The zero-crossing-counter processor was analyzed in some detail. Other workers have expanded on this good foundation, and much comparison of particular measurement techniques has been done. M. B. Histand et al. at the Colorado State University have reported on their research covering several aspects of ultrasonic measurements of hemodynamic phenomena, including detailed

---

*References are listed at the end of the report.

performance evaluations of certain instrumentation and testing methods.[2] Histand's work is directed toward the practical application of modern digital data-processing techniques to the CW Doppler ultrasonic blood-flow method.

As shown by Brody, the mean Doppler frequency is the mathematically correct parameter to be used in calculating blood-flow velocity. It is clear from Brody's analysis that the Doppler spectrum is quite dependent on the transducer/vessel geometry, and that large statistical fluctuations in the spectra will make accurate measurements difficult. Figure 2 shows the theoretical dependency of the spectral shape on the transducer's size and its orientation to the blood vessel. Note that if the projected transducer size (q_w) along the vessel is larger than the vessel diameter, the spectrum becomes nearly uniform and the mean Doppler frequency is equal to the mean flow velocity in the vessel. This single parameter, $\bar{f}$, is obtained from the spectral-density function F(f) via the relationship:

$$\bar{f} = \frac{\int_{-\infty}^{\infty} f \cdot F(f)df}{\int_{-\infty}^{\infty} F(f)df}$$

which can be recognized as a first-moment calculation.

The error that accompanies the above calculation is a function of the integration interval, which, by practical considerations, must be short compared with the pulsatile blood-flow dynamic period. Since the Doppler signal results from a process that involves large numbers of scatter points having both ordered and random velocities (especially for turbulent flow), it is obvious that the spectra will also have a random component that will make the ordered flow estimate be in error. An appropriate expression for the fractional accuracy developed by Brody is:

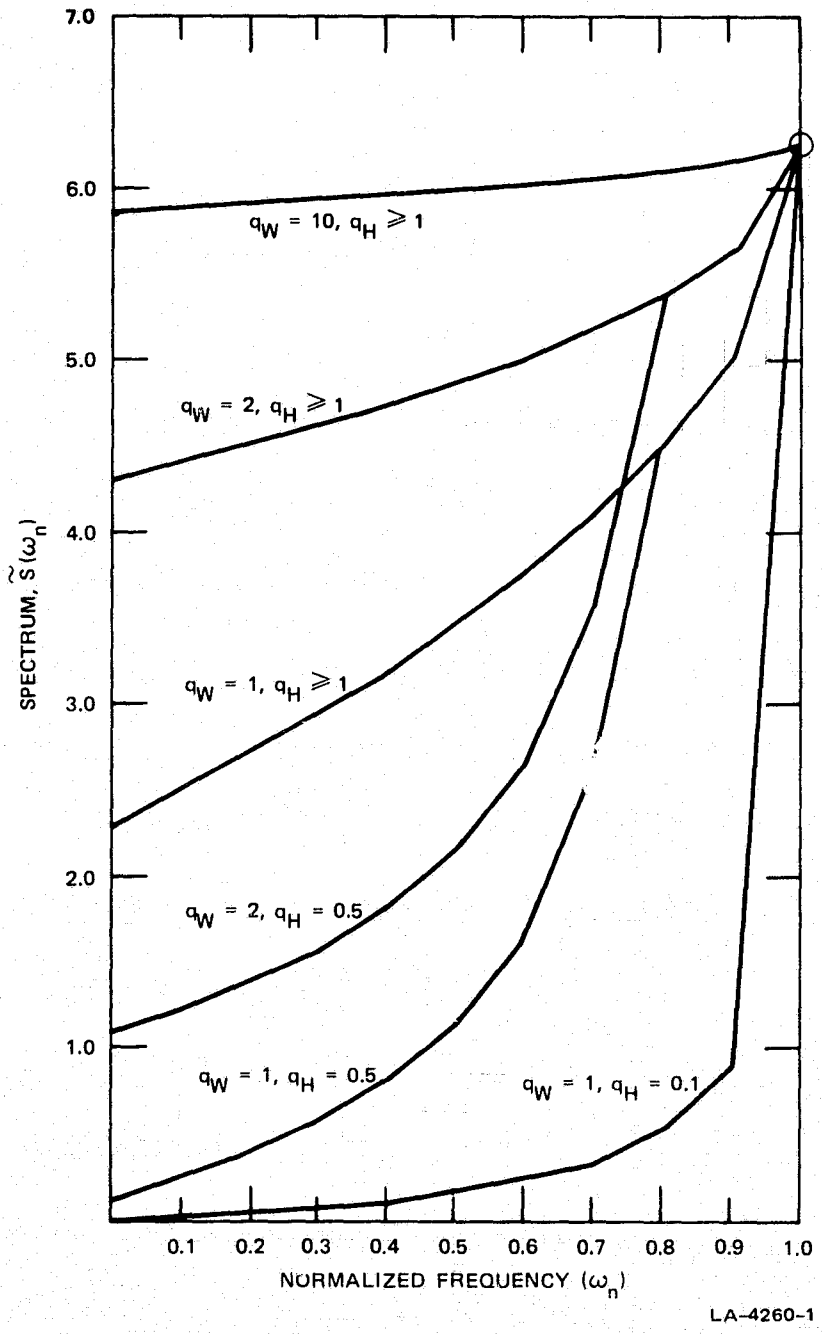

FIGURE 2 THEORETICAL DOPPLER POWER-DENSITY SPECTRA (normalized)

$$\frac{\sigma}{\bar{f}} = \frac{4}{3W_s T}$$

where σ is the standard deviation, $\bar{f}$ is the mean, W_s is the spectrum width, and T is the time waveform duration. For example, if the Doppler spectrum were 3 kHz wide (typical for transcutaneous signals from a major artery) and the transform time duration were 10 ms (to provide adequate pulsatile flow time resolution), then a single first-moment frequency estimate would have an rms statistical error of 21%. Subsequent smoothing of a set of estimates will further reduce the fluctuations by the square root of the integration period relative to the spectra period. For example, if a 100-ms integration were used, the pulsatile waveform fluctuation would be reduced to about 7%, a value not unreasonable for such measurements.

As Brody points out, the only way to improve the measurement accuracy for a given time integration is to increase the spatial integration by illuminating the blood vessel more uniformly, but this must be traded off for Doppler bandwidth. Thus, there is an optimization task that must be performed relating transducer size, aspect angle, and vessel size and depth.

The ZCC is used extensively in blood-flow velocity measurements primarily because of its simplicity and relatively good performance. Basically it is, just as its name implies, a circuit that generates a voltage analog of the zero-crossing density of a quasi-periodic signal by integration in the output low-pass filter. Since the input waveform is noise-dominated and its amplitude is not used explicitly, the circuit responds to the dominant spectral-energy component, not to the average. An analysis given in Brody's thesis showed that for a Gaussian random waveform, the ZCC actually computes the square root of the second moment of the power spectrum. Thus it is clear that any broad-spectrum signal

similar to the Gaussian one will result in some error between the ZCC output and the desired first-moment calculation, and the amount of the error is dependent on spectrum shape. Obviously the two methods tend to merge to the same value as the signal spectrum narrows to quasi-CW shape, but any skew in the spectrum implies an error between the two measurement methods. For qualitative purposes the ZCC is very cost-effective and, if only moderate quantitative accuracy is required, it can be used in some applications.

V EVALUATION OF EQUIPMENT

As outlined in the previous sections, the ultrasonic CW Doppler flow-measurement technique results in a received signal that is composed of the desired Doppler-shifted blood-scatter signal and the unavoidable direct CW signal that leaks or couples in from the transmit element via the transducer support material, electromagnetic coupling, skin reflections, and subcutaneous tissue backscatter. The early flowmeters use the entire signal and convert it to audio by use of the simple envelope detector. This type of detection is incoherent--i.e., the sense of the Doppler-shifted blood scatter signal is lost, so the instrument is nondirectional. Otherwise the method is simple and relatively sensitive. The output from the detector is applied to a zero-crossing detector (a clipping amplifier) followed by a simple frequency-to-voltage converter and a smoothing filter. This combination, called the zero-crossing counter (ZCC), then estimates the most likely frequency of the Doppler signal, thus providing a continuous analog voltage for use by the investigator.

To provide bidirectional flow-indication, the newer L&M Electronics Inc. flowmeters employ synchronous detection whereby a portion of the transmitter signal is used as the local oscillator (LO) frequency to mix with the received signal and yield the difference frequencies corresponding to the Doppler shift. Two channels in time-phase quadrature are used as shown in Figure 3, involving two mixers and two LO signals that differ in phase by 90 electrical degrees. One channel uses a ZCC to generate the flow-velocity estimate, as in earlier flowmeter designs. The flow direction is determined by comparing the phase of the signal output from the second channel with that of the first, and the result is

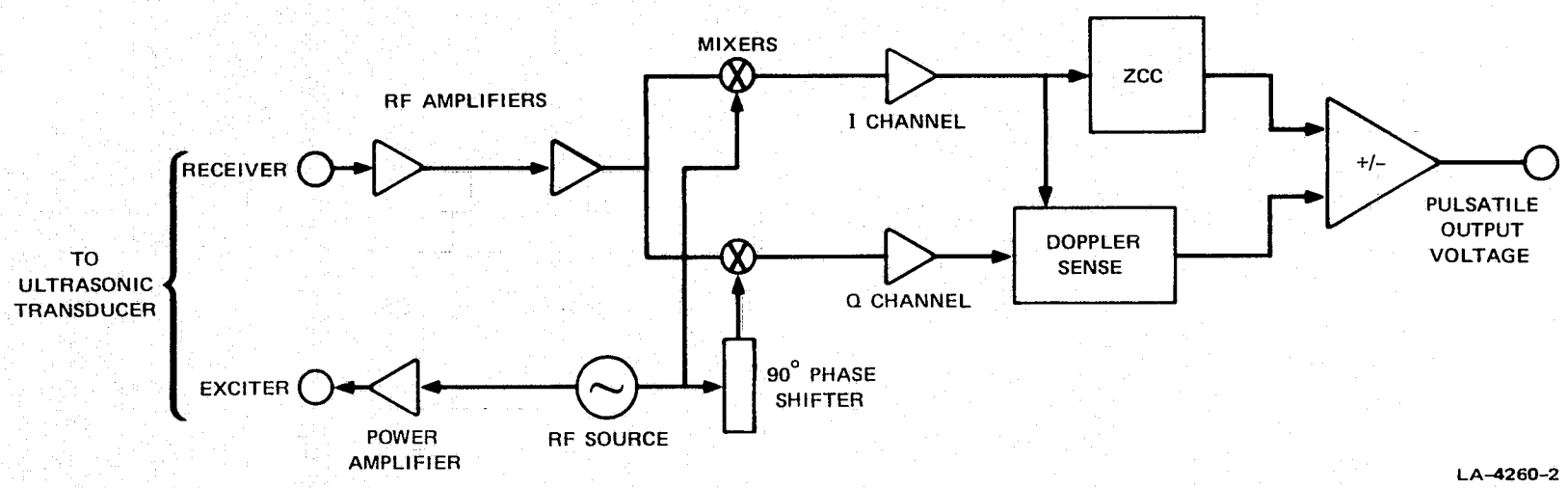

FIGURE 3 SIMPLIFIED SYSTEM BLOCK DIAGRAM — L&M DOPPLER FLOWMETER MODEL 1012

used to steer the ZCC output either positive or negative to indicate the flow direction. This output is then the analog of the instantaneous or pulsatile blood-flow velocity, which is linearly proportional to blood-volume flow rate. However, the use of the ZCC introduces the same sensitivity and accuracy limitations as in the earlier instruments.

As part of this investigation, SRI was asked to evaluate and, if appropriate, suggest improvements to the Doppler flowmeter manufactured by L&M Electronics Inc. This unit and its companion versions represent nearly the state of the industry in modern all-solid-state electronics and packaging techniques as applied to the bioengineering field. It is small, lightweight, self-powered, and portable. Circuitry is relatively straightforward but draws upon many of the new integrated linear and digital chips and forms a nearly optimum mix of modern linear and digital techniques. Electrical performance is very good, with basic sensitivity only slightly poorer than is achievable by a perfect noise-free ideal. There are some engineering tradeoffs that have been made for the sake of size and cost, but these are acceptable.

Appendix A presents the details of the electrical performance evaluation for the L&M Model 1012 flowmeter. Only a couple of specific design and adjustment suggestions were made, with the main object of improving the sensitivity and suppressing abnormal response conditions. These suggestions were subsequently incorporated into the unit by L&M, and the hoped-for results were realized. It is felt that this instrument is now a good base-line for comparison of any new CW Doppler flowmeters or techniques, with the stipulation that transducer characteristics be related to the input/output impedance of the instrument. Since the exciter source impedance is low (about 5 ohms resistive) the power delivered to the illumination (transmitter) transducer is dependent on the load impedance. Similarly, the effective noise figure, and hence system sensitivity, of

the instrument is affected by the receiver transducer impedance. In other words, any comparison must allow for normalization of such variables as those mentioned above before a final evaluation judgment can be offered.

A second equipment-evaluation task was a short test of the older nondirectional flowmeter used by NASA-Ames, also built by L&M Electronics Inc. During high-G stress testing of human subjects on the NASA centrifuge, it was observed that the nondirectional flowmeter seemed to provide a better sensitivity than the newer directional unit. Also, different transducer probes that seemed to provide consistent results using the new directional unit gave inconsistent results on the older nondirectional unit.

Basically it was found that the performance differences could be explained in terms of the different types of detectors used in the two flowmeters. The new unit employs coherent signal conversion to audio, which is a completely linear process, while the older design uses the more simple envelope (diode) detector, which is basically nonlinear and signal-level-dependent. Also, the older unit allows for operator adjustment of the ZCC threshold, and its preprocessing bandwidth is 3 kHz, vs the 10-kHz bandwidth of the newer unit. These differences were adequate to explain the apparently better sensitivity of the older unit. The problem of anomalous performance with different transducers in the older unit was found to be simply a question of the relative level of the leak-through carrier level. An envelope detector will operate as a linear detector only if there is a "carrier" of sufficient level and if the detector element itself is close to a perfect rectifier. A diode that is biased and not linearized by use of series resistance is intrinsically nonlinear, and has a voltage/current transfer function that is approximately exponential at low carrier levels, making its conversion gain dependent on the level of the carrier signal.

Thus, if the direct or non-Doppler signal is much larger than the scattered Doppler signal, the diode detector provides adequate conversion gain and reasonable linearity. However, if the carrier is significantly lower for some reason, then the detector's conversion gain is proportionately reduced and spectral distortion of the Doppler signals can occur. Apparently newer transducer sensors that include an absorptive "fence" between the transmit and receive elements yield a significantly smaller coupled-carrier level, so that detected output signals appear lower in amplitude; this corresponds to poorer sensitivity. In effect, the older nondirectional flowmeter is transducer-dependent. Appendix B includes the details of this measurement and equipment evaluation task.

VI ADVANCED DATA PROCESSING

The output voltage from the Doppler blood flowmeter is an analog of the pulsatile (instantaneous) blood flow rate. Because this analog is generated in a circuit (the ZCC) that does not calculate the mean velocity of the Doppler signal, there will be errors introduced that are dependent on the signal spectral shape. Also, since the ZCC must operate on the folded spectrum and includes a noise threshold margin, a loss in sensitivity occurs. Digital processing has the potential for improving the ultrasonic CW Doppler technique over that obtainable using the ZCC, and the following text attempts to define that potential by showing typical signals from the two techniques over a range of noise conditions.

Applying modern digital data-processing methods to the Doppler blood-flow measurement involves several steps and certain conditions. Data format is the first subject that must be covered. Basically the Doppler signals of interest are generated at the ultrasonic frequency of the probe signal, but because of the small-percentage frequency shift, they can be frequency-translated to any other center frequency. Since the maximum absolute Doppler shift is less than 10 kHz either plus or minus from the probe signal frequency, it is advantageous to translate the entire frequency band down to the audio band. This can be done in either of two ways. First the entire Doppler band could be offset by one-half its total and then translated to the audio band. For a maximum Doppler shift of plus or minus 10 kHz, the translated band would range from zero to 20 kHz. Doppler sense is completely preserved, but there is an offset that must be considered. The other method is to simply split the Doppler band into orthogonal in-phase and quadrature-phase components (I and Q) and then translate directly to zero frequency, which "folds" each set

symmetrically. Although neither the I nor Q component alone can give the Doppler sense, the appropriate combination of the two can do so. The advantage of the second method over the first is that the Doppler frequency ranges naturally from zero to its maximum value directly, and each channel bandwidth is just half the total. The disadvantage is that two channels must be used with identical noise, dynamic range, gain, and phase characteristics over the data bandwidth.

Since each method yields the same final results, it is simply a question of equipmental convenience that determines which is to be used. The older nondirectional flowmeters were by necessity zero-frequency conversion systems, so it was a natural evolution to expand that format into the I-and-Q two-channel configuration for Doppler sense determination. This is what is done in the new L&M Doppler flowmeter with hybrid analog-and-digital processing to extract the Doppler sense. Fortunately this format is also appropriate for use with the all-digital processing method, since Fourier transforms are available in both the real and the complex input format. Also, it is not difficult to digitally sample and encode simultaneously at audio rates commensurate with the flowmeter data bandwidth. The discrete Fourier transform as implemented via the FFT operates on a pair-set of 2^n complex time samples to form a new pair-set of 2^n complex frequency components. The power spectral density (PSD) is then calculated from those complex numbers. Dynamic range of the PSD is related to the original time-data quantization size and the number of points in the transform set. Dynamic range is usually expressed as a "processing gain," which relates to the maximum effective enhancement of a coherent signal buried in Gaussian white noise and is simply 2^n. Frequency resolution is similarly related to the data set and is calculated from the time length of each transform. Thus, if the sample length is T seconds, the frequency resolution is 1/T Hz. Of course the digital sampling rate must

be commensurate with the data bandwidth, and according to the familiar Nyquist criterion, must be at least twice as much as the data bandwidth.

Figure 4 shows the general equipment block diagram for the sampling of data provided by the L&M directional Doppler flowmeter. Key parameters of this system are listed in Table 1. Since a real-time complex FFT computer was not available for this data-processing demonstration, it was necessary to convert the data streams, format them in standard IBM form and write them on standard digital tape for later playback into a general-purpose computer facility. It should be remembered that the FFT can be implemented in hard-wired logic for such specialized data processing jobs and all of the subsidiary computations and control can be done in a small microprocessor--all in real time.

Representative data sets were generated under controlled conditions using a standard NASA-Ames transcutaneous ultrasonic transducer probe with the aid of a NASA-Ames representative who was familiar with the procedures for taking such physiological data. Principal data were obtained from the blood flow in an artery with the subject inducing both normal unidirectional blood flow and representative reverse blood flow under partial stress conditions. Several data sets were generated in an attempt to simulate "good," "fair," and "marginal" signal-to-noise-ratio (SNR) conditions that have been experienced during the actual NASA-Ames Centrifuge G-stress test series. Since one of the objectives of the test is to ascertain the benefit of spectral processing, such a controlled data degradation was necessary. The pulsatile analog output voltage from the L&M flowmeter (see Figure 3) was also digitized (at a much slower rate) in parallel with the unprocessed audio signals for comparison with the digital processed results. The instrument controls were set for a representative case that is often used during testing with the flowmeter, so that a good comparison of the digital processing result could be made.

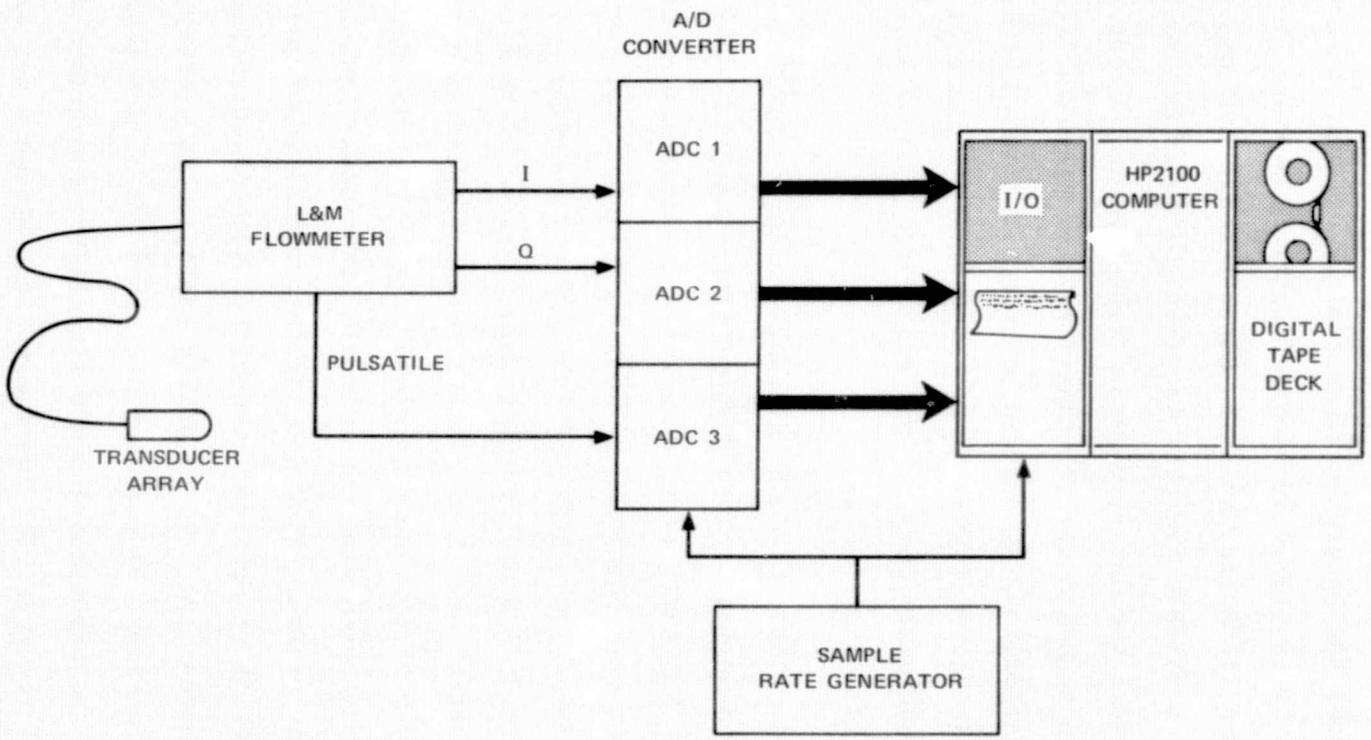

FIGURE 4 BLOCK DIAGRAM OF FLOWMETER SIGNAL DIGITIZATION EQUIPMENT

Table 1

SALIENT PARAMETERS OF DIGITIZATION SYSTEM

Sample rate	10 kHz
Sample resolution	8 bits
Tape block size	2048 words
Tape format	9-track IBM-compatible
Total data rate	161 kbits/s

The actual processing of the digitized signals was performed on a general-purpose computer facility so that economy and flexibility in program development and testing could be achieved. Program flow is illustrated in Figure 5. The first operation, of course, is the separation of the time values into blocks of 2^n voltage pairs for transform via the FFT subroutine. This results in a new set of 2^n real and imaginary frequency components, which are then combined to produce the unfolded PSD. These values are then processed to extract the desired parameter, and this parameter is used to form the pulsatile velocity time waveform.

Initial spectral analysis of some earlier data obtained from analog tapes supplied by NASA-Ames from one of their centrifuge tests indicated that the peak of each of the spectral estimates might be an acceptable analog representation of the average flow velocity if the fluctuations in the frequency domain were reduced by smoothing. The theoretical spectral shape for typical transducer/vessel geometries indicates that such an approach should work. However, when the spectra are essentially flat, the peak is not well defined and fluctuations would be expected to make such an algorithm of little value. For some cases tested it was found that the spectra in general were somewhat rounded and did display a definitive peak, so that after smoothing in frequency the peak estimate

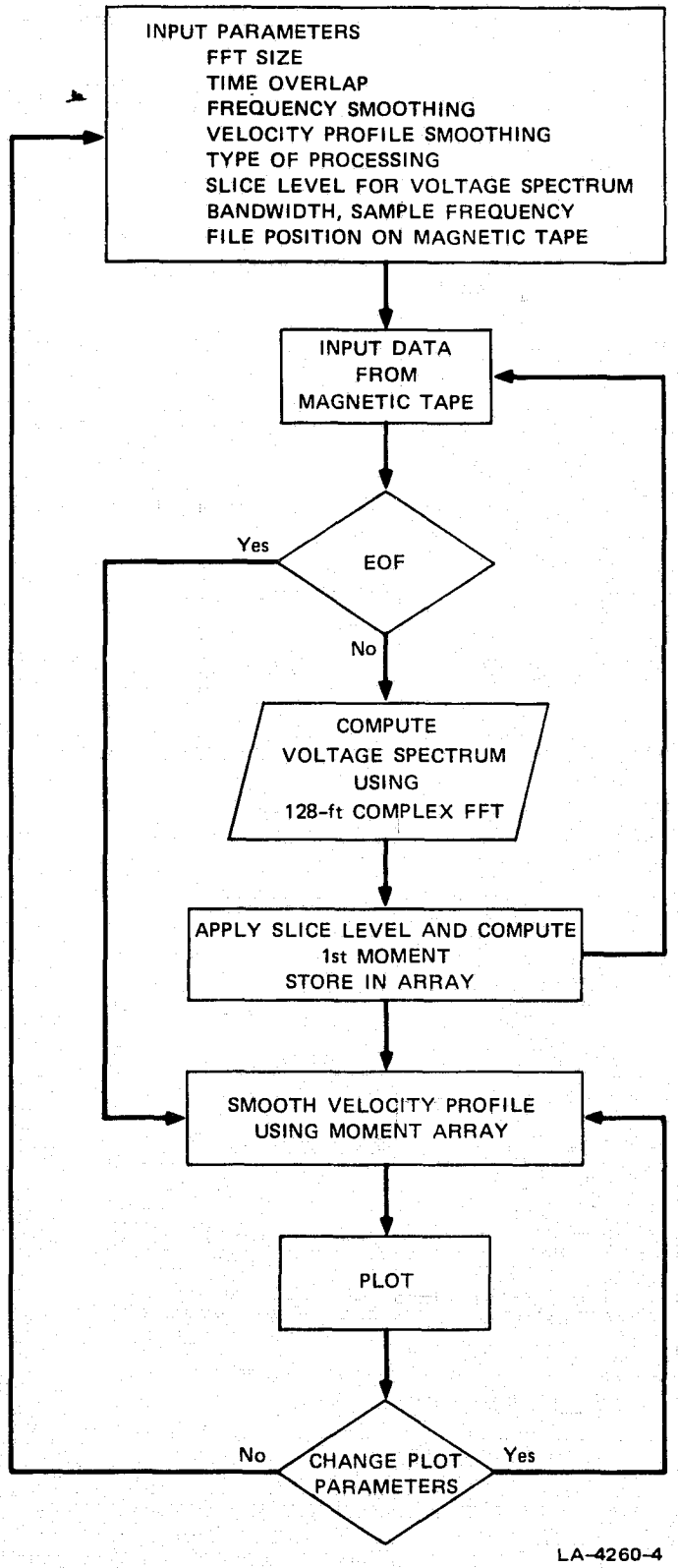

FIGURE 5 DIGITAL PROCESSING FLOW DIAGRAM

was not too much different than the true mean estimate. Unfortunately, as the SNR decreased, the peak estimation degraded much faster than the mean estimation. Also, for other data collected under different conditions or from different subjects it was found that the spectral shape changed sufficiently during the pulsatile period so that the peak estimate resulted in excessive fluctuations. Thus in general the peak estimation algorithm, although conceptually neat, is not appropriate for the mean blood flow velocity measure. Also, it is not much more efficient in terms of computational complexity or speed because it requires spectral smoothing in the frequency domain.

The mean or first-moment calculation was found to be effective, but it was necessary to apply it to the power spectrum, not the voltage spectrum. This was especially true for low-SNR conditions where uniform noise across the spectral window tended to bias the integration either to zero for the double-sided spectra or to one-half the frequency band for non-directional single-sided spectra. Mean estimates derived from higher-order spectra would not be appropriate for two reasons: One, the physical interpretation would be artificial and not in agreement with the theoretical analysis, and two, it would tend toward the previously mentioned peak estimation technique, which was found to be too sensitive to spectral shape. Thus we have limited ourselves to first-moment calculations of the PSD.

Figure 6 is a representative PSD for a 12.8-ms data set from the L&M flowmeter while measuring pulsatile blood flow. This spectrum is for a good SNR (greater than 30 dB), and is taken at about the peak blood flow velocity. Note that the spectrum is very noise-like but has a general wideband shape from zero frequency (really the instrument's high-pass filter limit of about 500 Hz) up to several kilohertz. Some small degree of spectral fold-over is visible and can be attributed to minor and unavoidable amplitude and phase inaccuracies in the L&M dual-channel

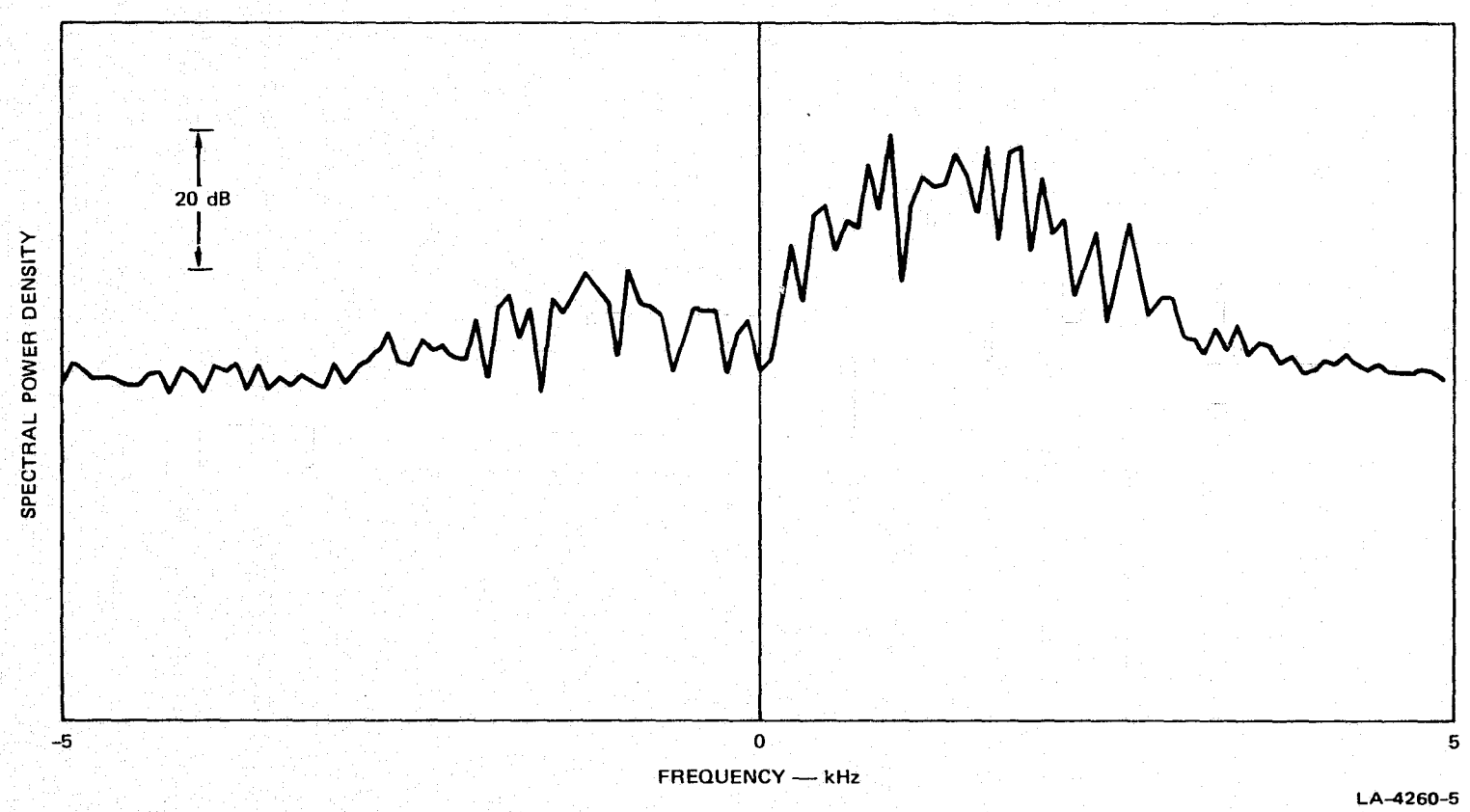

FIGURE 6 REPRESENTATIVE DOPPLER FLOW SPECTROGRAM

circuitry. The important feature to be noted is the large fluctuations in the spectral values. These are not noise-induced but are intrinsic properties of the Doppler scattering mechanism and can be seen in similar data independent of SNR. This is the basic problem that makes the average-flow-rate calculation difficult for either the analog or the digital processor.

As an aid in visualizing the time dynamics of the Doppler signal, a sequence of PSDs have been assembled in Figure 7. Time increases from bottom to top in 12.8-ms increments and shows how the flow pulse forms rapidly (within 30 ms) and then decays more slowly back to the quiescent conditions. Actually there is slow flow prior and subsequent to the main flow pulse, but the L&M flowmeter high-pass filter tends to suppress it. Remember that the vertical scale of each PSD is logarithmic, with 30 dB (1000:1) between adjacent spectra. If plotted on a linear vertical scale (linear in power) the base-line noise would be completely suppressed and only the largest of spectral components would be visible.

Processing of these data sets using the mathematical algorithm of the normalized first moment is the next step in the digital calculation. Figure 8 shows a short section of the constructed pulsatile flow without any smoothing applied to suppress fluctuations. Basically the effective bandwidth is just that of the PSD, and in this case is about 80 Hz. Noise fluctuations are visible on the base-line when no flow signal exists, but they are not excessive. In general, some amount of additional filtering is desirable, and the case at hand is usually less than 10 Hz. Figure 9 shows the results when the calculated pulsatile data are smoothed by use of a sliding 7-point triangular function that synthesizes a low-pass filter with a 9.8-Hz corner frequency. This appears to be a very reasonable facsimile of the pulsatile flow and certainly is as good as the ZCC results. Figure 10 compares a longer segment of pulsatile flow waveform

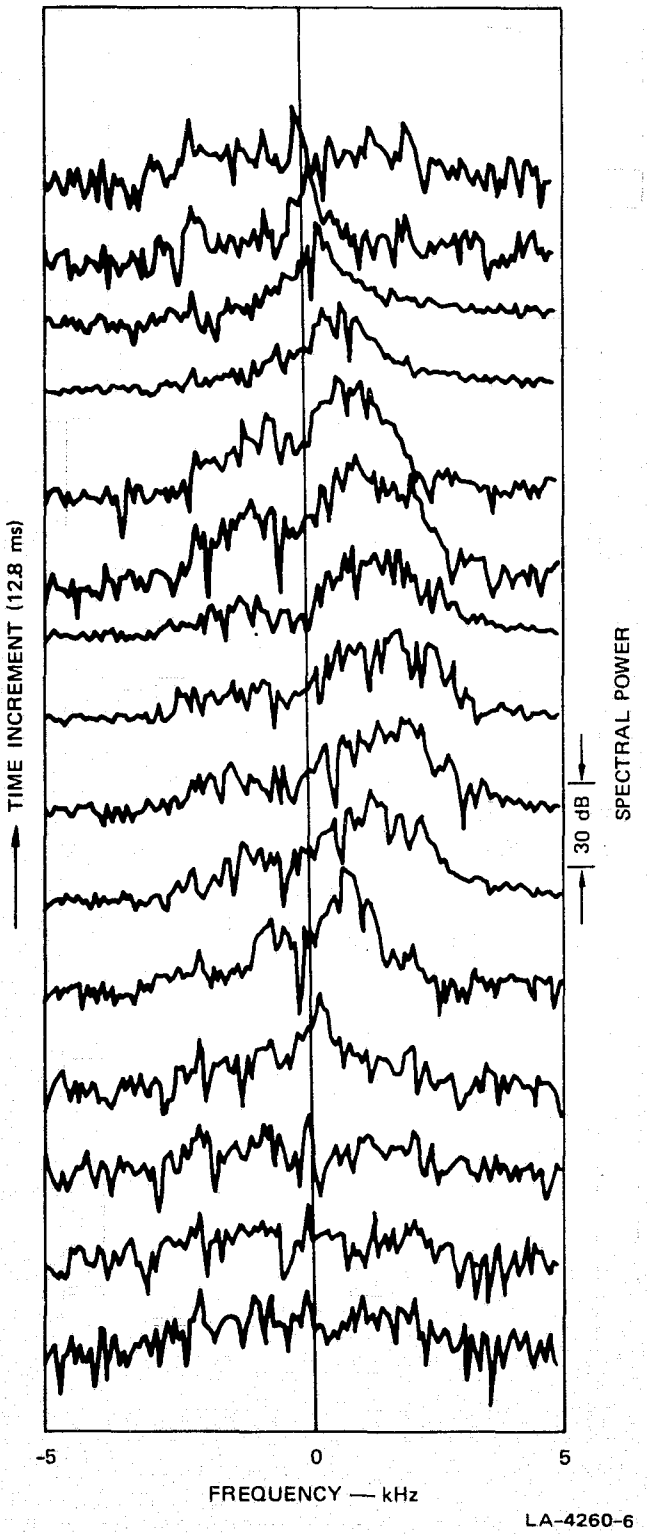

FIGURE 7 BLOOD-FLOW-SPECTRA TIME SEQUENCE

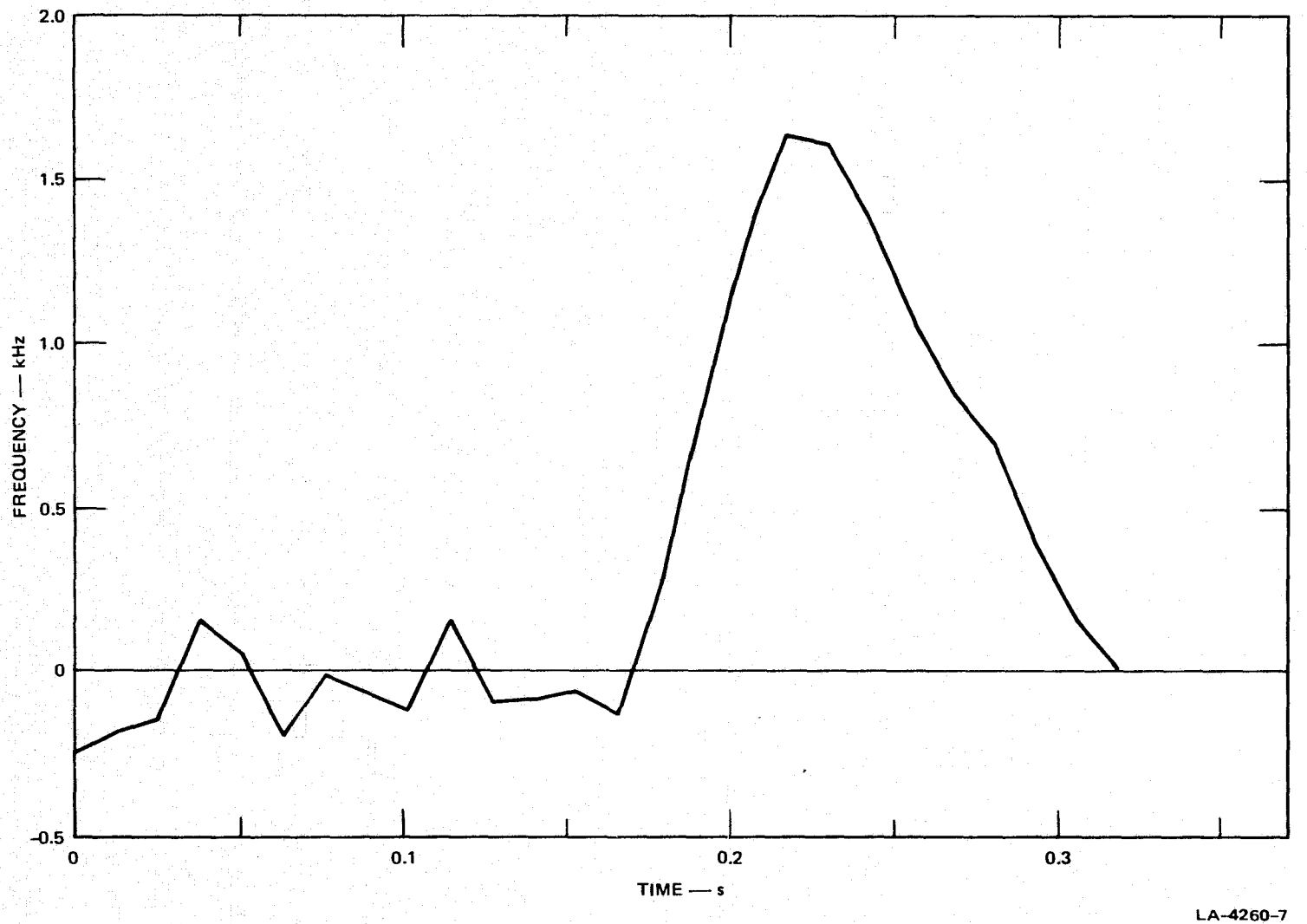

FIGURE 8 DIGITAL FIRST-MOMENT ESTIMATE OF PULSATILE WAVEFORM

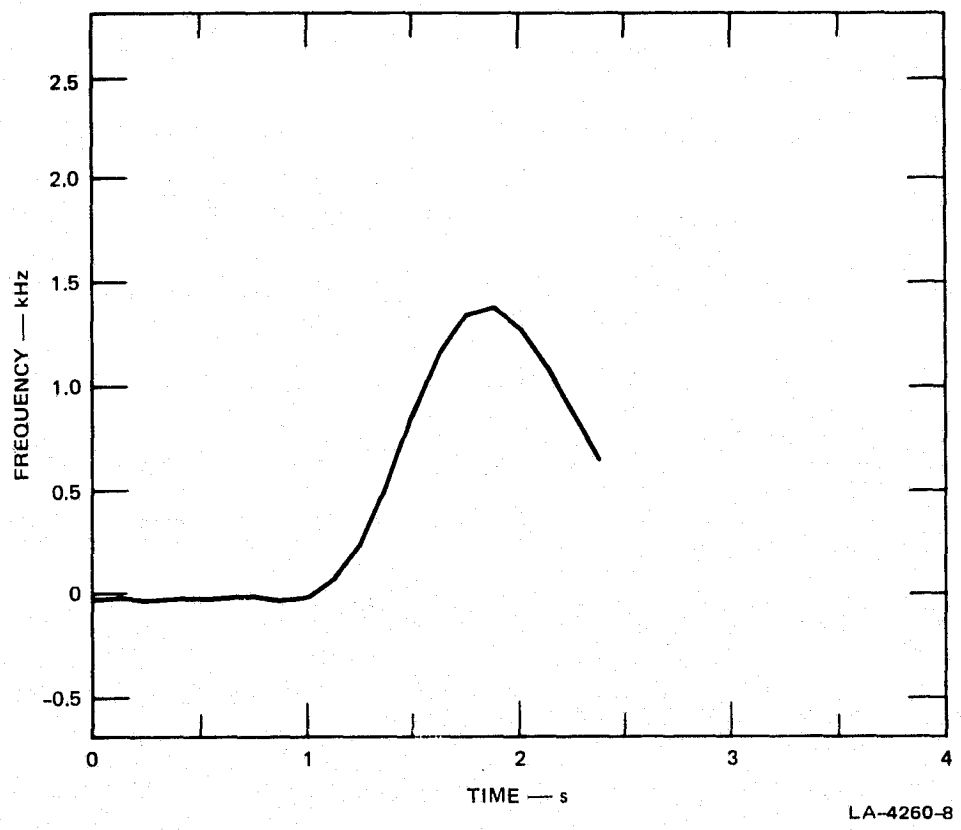

FIGURE 9 DIGITAL FIRST-MOMENT ESTIMATE OF SMOOTHED PULSATILE WAVEFORM

for both the analog ZCC result and the computer-calculated version. It would be difficult if not impossible to distinguish the two without labeling.

The analog ZCC pulsatile processor includes a hold-off or hysteresis in the signal zero-crossing detector that is necessary to keep the system noise from generating excessive pulsatile fluctuations when the flow is low or nil. In the older nondirectional flowmeters this threshold was manually adjustable and the operator was able to choose how much noise could be allowed on the pulsatile output. In the newer directional units this threshold is fixed at a level about three times the average audio noise to minimize fluctuations. In contrast, the digital processing method does not require any equivalent type of noise thresholding or

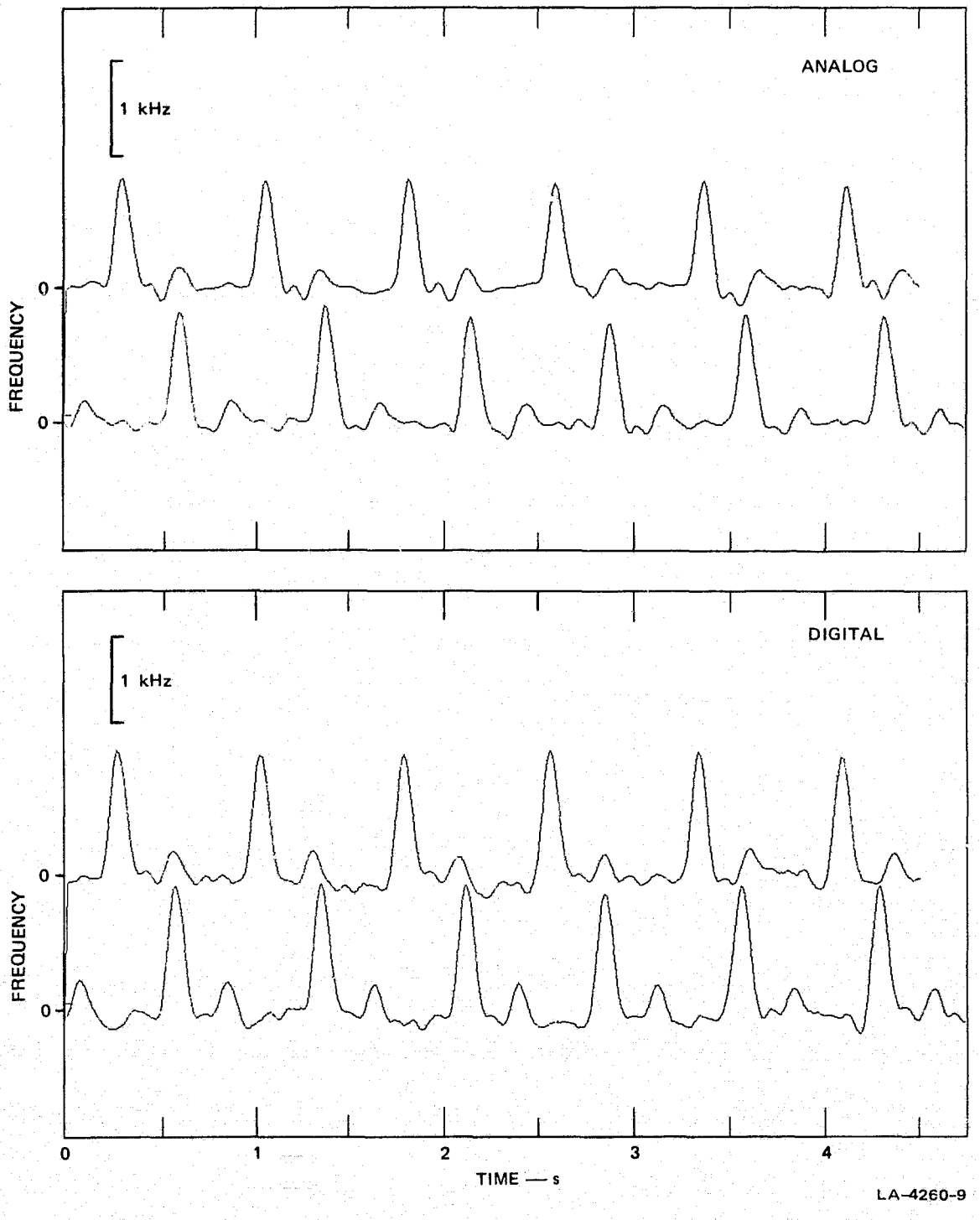

FIGURE 10 COMPARISON OF ANALOG AND DIGITAL PULSATILE WAVEFORMS, SNR > 30 dB

slicing. The mean estimation of the PSD employs integration across the entire double-sided frequency space, which smooths nicely to zero with some statistical fluctuations. Further smoothing of the pulsatile estimate values reduces those fluctuations to an almost insignificant amount.

Since the threshold or slice level is about 10 dB above the noise for the ZCC, it was expected that a similar improvement in sensitivity could be achieved with the digital processing. To test this hypothesis, a slice level was applied to the PSD data sets prior to the mean estimation. To be consistent, the level was also set 10 dB above the spectral noise level when no flow signal was present. This level corresponds to the ZCC hysteresis minus the FFT processing gain. All spectral-estimate values below this level are then replaced by this level. Figure 6 shows the slice level drawn on the spectrum while Figure 11 shows the effect on the calculated pulsatile waveform. As expected, the low-level noise is removed while the signal is unaffected. Similarly, just as for the ZCC, this slice operation results in a degradation for low-SNR conditions.

Let us take a look at the results for the other controlled data sets taken on the L&M flowmeter and digitized for processing. As outlined before, three sets of "controlled degradation" pulsatile flow data were generated. The first and best SNR was just presented on Figure 10. The second set, which we call the fair data, is shown on Figure 12 and illustrates the slight but noticeable difference between the analog pulsatile waveform and the digital. Both have the same bandwidth (about 10 Hz), but the digital-generated set did not include any slicing. If one cares to speculate on the differences, it might be said that the digital waveform seems to exhibit more (and possibly better) detail at the lower flow rates. However, this conclusion is still open to question, in the absence of a controlled calibrated flow measurement. The third and nominally marginal data set is shown on Figure 13. Here we see a marked difference

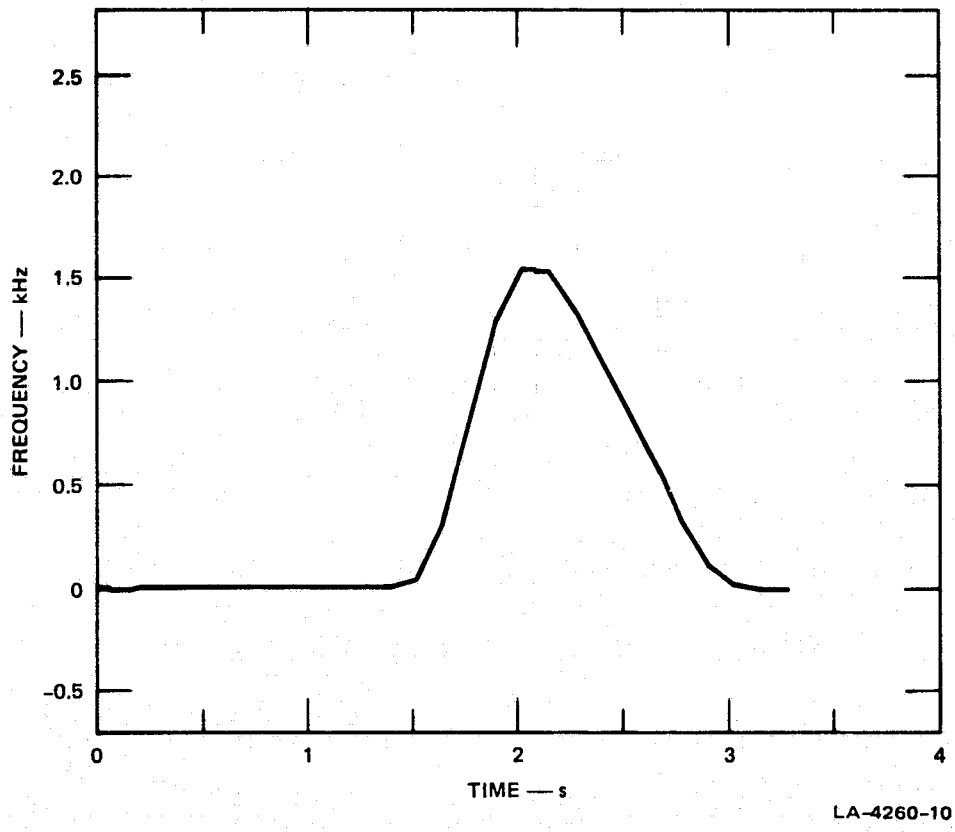

FIGURE 11 DIGITAL FIRST-MOMENT ESTIMATE OF PULSATILE WAVEFORM, -45 dB SLICE

between the analog and the digital representations, where it is not unreasonable to say that the digital results appear better. Both low-level and peak flow estimates seem to be better defined, which one would intuitively expect, knowing the two processing methods. Apparently the digital processing without slicing indeed does have better sensitivity, since it uses all the available information. Indeed, if the digital processing is repeated with slicing, the results are degraded and almost overlay the analog waveforms.

As an aid in understanding the audio Doppler signals being processed, refer to Figure 14. Here we have portions of the three comparison-test data sets plotted out in raw audio signal voltage form. As is obvious, the top trace is the good SNR set where each piece of the blood-flow

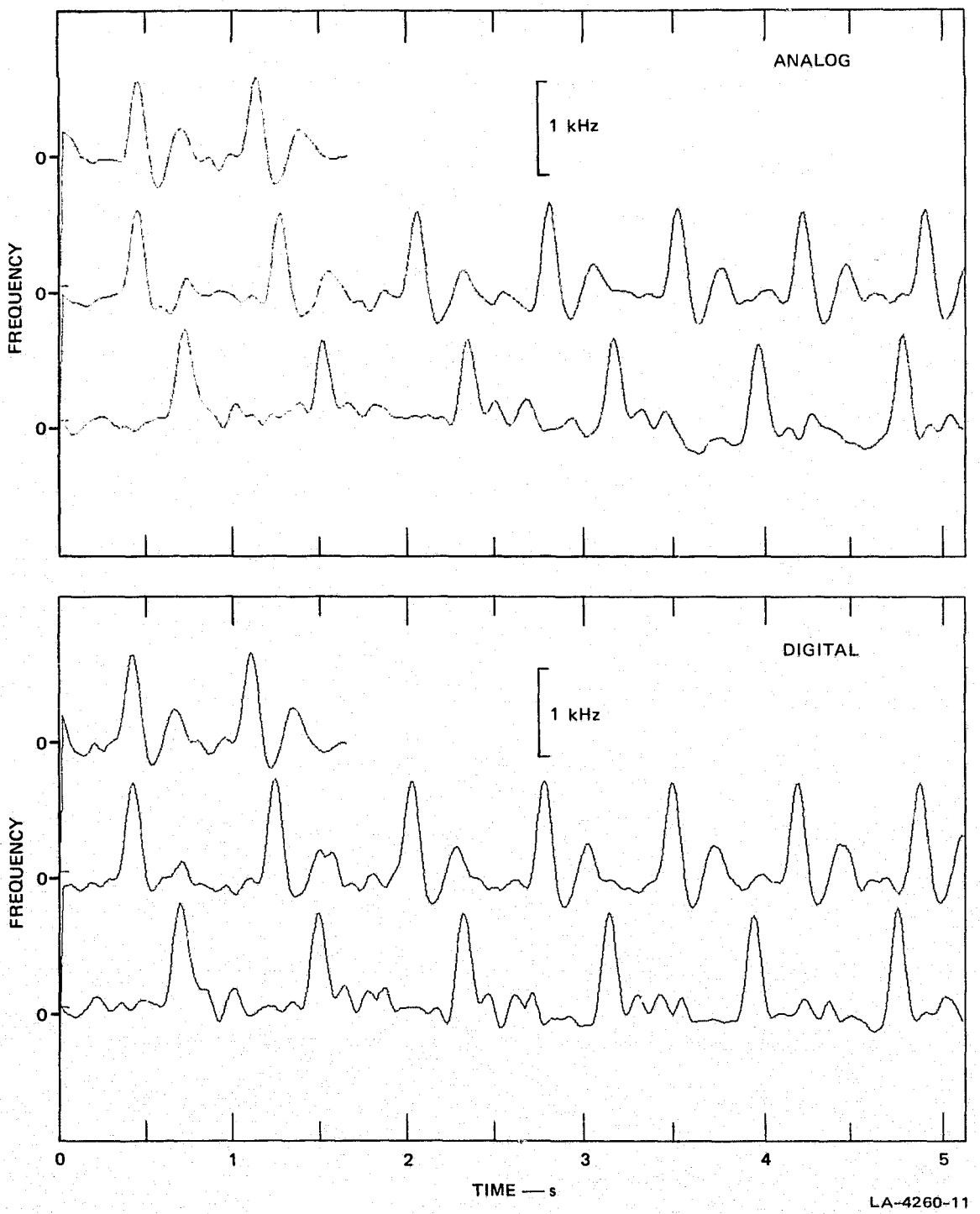

FIGURE 12 COMPARISON OF ANALOG AND DIGITAL PULSATILE WAVEFORMS, SNR ≈ 20 dB

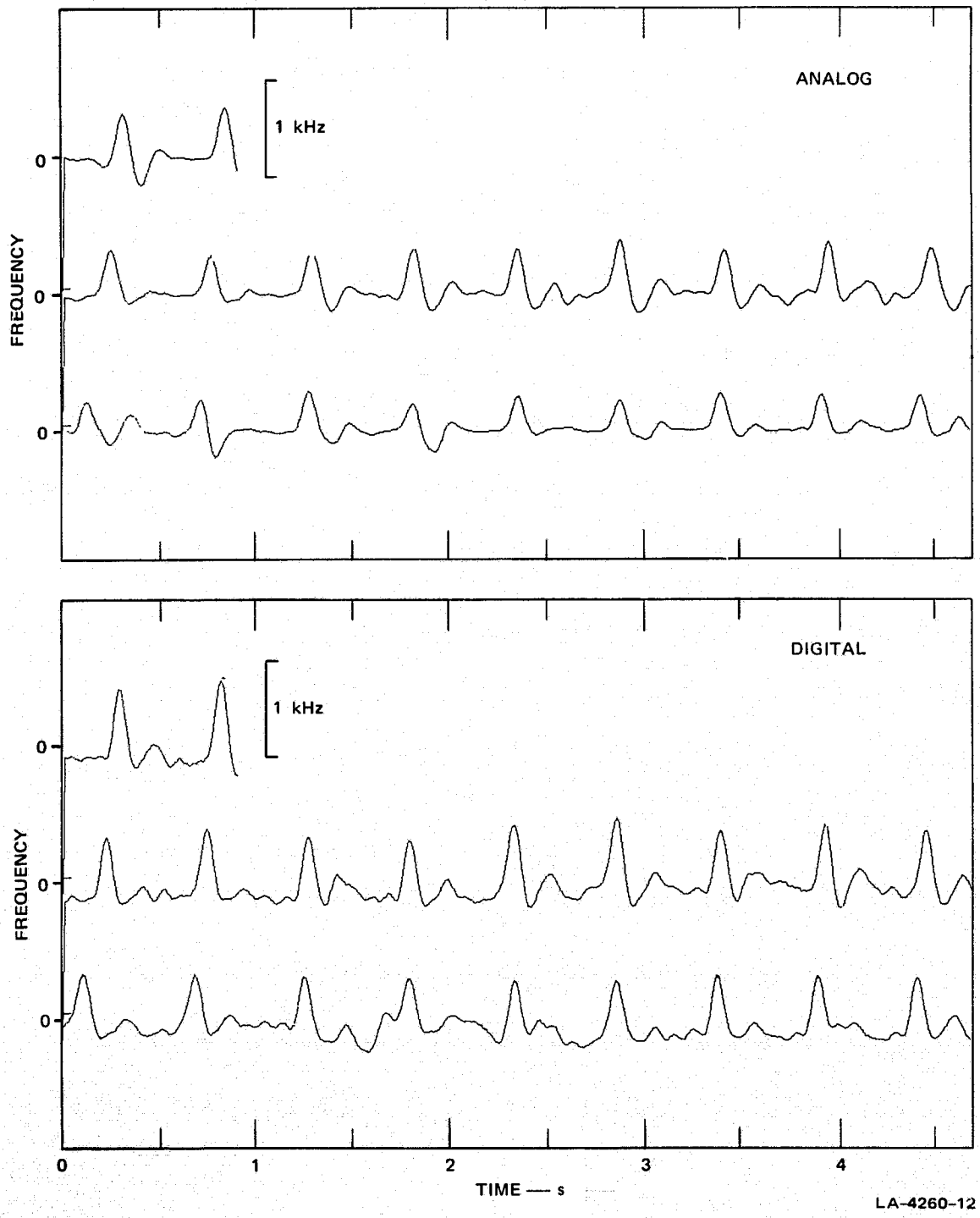

FIGURE 13 COMPARISON OF ANALOG AND DIGITAL PULSATILE WAVEFORMS, SNR ≈ 10 dB

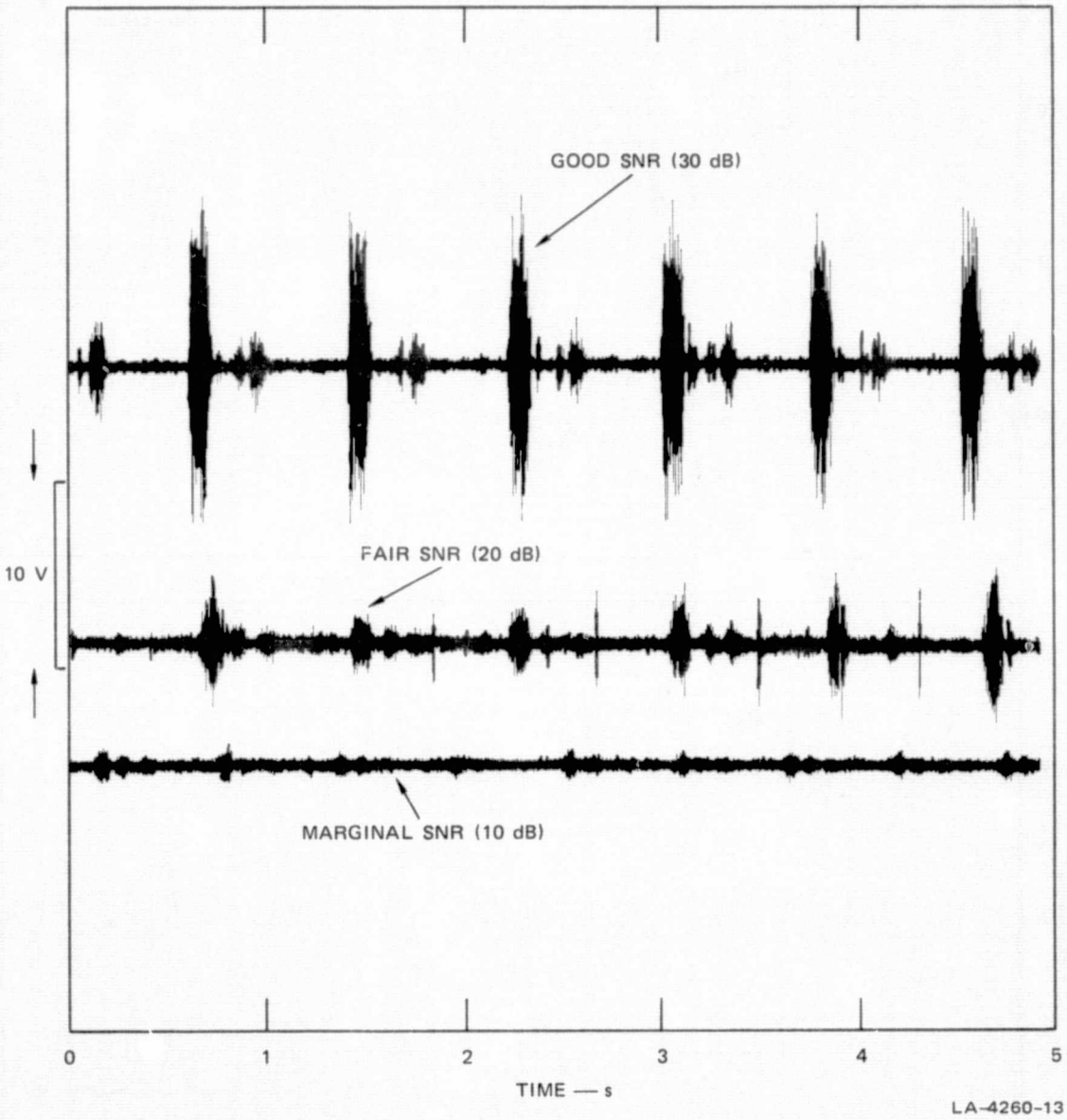

FIGURE 14 COMPARISON OF DOPPLER AUDIO-SIGNAL TIME WAVEFORM

Doppler signal can be observed. This voltage waveform can be compared directly with the pulsatile waveforms on Figure 10 and corresponds to the first 5 seconds of the data set. The second audio voltage signal is for the fair SNR set, which still is quite recognizable and corresponds nicely with the companion pulsatile data shown on Figure 12. The marginal SNR voltage trace indicates that a 10-dB SNR is really not much, and it is somewhat surprising that such good pulsatile waveforms are produced by the ZCC and the computer algorithm on Figure 13.

VII INVESTIGATION OF TRANSDUCERS

As an aid to understanding the entire CW Doppler blood-flow problem, a review of the state of the art in ultrasonic transducer design and fabrication techniques was made, and the review was then applied to the job of improving the current transducer sensor arrays used in the CW Doppler blood flowmeter. Since the Ultrasonics Laboratory of SRI has been involved in exactly this kind of endeavor for several years, it was natural to simply call upon their in-house expertise for this task. This work was restricted to a straightforward analysis of a representative pair of NASA-Ames ultrasonic sensor arrays. Subsequently, one of the NASA units was modified in an attempt to fabricate a considerably improved version.

The principal thrust of the sensor evaluation was to discover just what is the performance for the NASA units and what fabrication or assembly technique improvements might be appropriate. The two sensor arrays were first electrically tested by use of a simple CW-pulse reflection method whereby the individual transducers are placed in a water bath, accurately aligned parallel to a monel reflector block a short distance away, and then excited with the pulsed-CW signal. The returned signal then described the two-way efficiency of the transducer element. By varying the frequency of the test pulse signals, the efficiency-versus-frequency behavior could then be obtained. The electrical impedance of the element was also measured with the element still immersed in water but not near the reflecting block. These parameters are necessary so as to be able to separate the impedance mismatch loss from the intrinsic energy conversion loss and extend the results to practical situations where source and load impedances are different.

Figure 15 shows the response curves for the transducer pair that make up one of the two subject sensors. Note that one chip has a relatively narrow-band response compared to the other, and that they do not overlap as might be appropriate. Thus it is obvious that this sample chip should have an overall poor efficiency as indicated by the product curve (less than 4%), but that in a system not limited by noise, this sample would provide adequate performance. In general, however, it would be better to match the frequency response of the two transducer chips for optimum efficiency and hence ultimate sensitivity under adverse user conditions. This recommendation was made to NASA-Ames and applied to subsequent sensor array fabrication procedures.

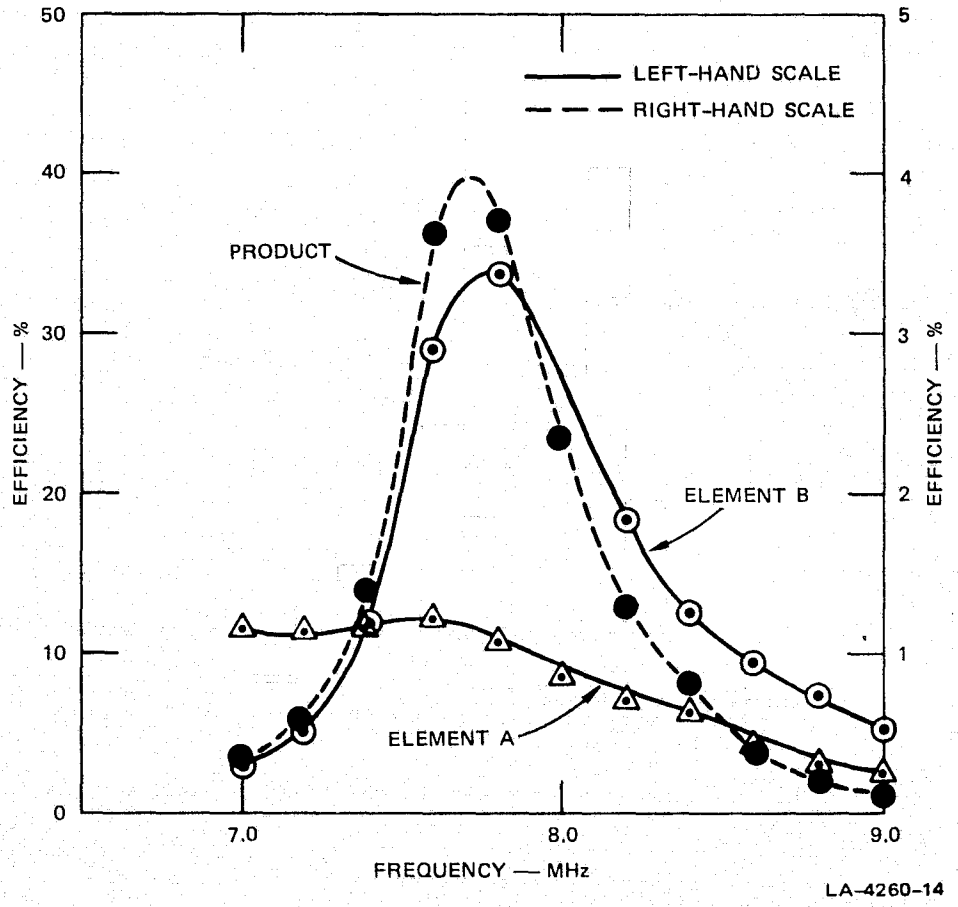

FIGURE 15 NASA-AMES TRANSDUCER — EFFICIENCY vs FREQUENCY RESPONSE

Data obtained for the second of the two array sensors tested exhibited an even greater difference between the frequency response of the two chips, and a much poorer overall efficiency. This is a unit that definitely would give inferior performance when used with the blood flowmeter and could be considered representative of the lower end of the production yield curve. Actually the two sensors used in the test evaluation had been "selected" by NASA-Ames to represent the two extremes of performance observed on many sensors up to this time, and were not randomly chosen out of a production batch. This selection enabled our analysis to quickly focus on the problems of immediate concern and result in useful corrective suggestions. The second sensor was then dissected to discover the reasons for the relatively poor performance. Several mechanically related fabrication errors were located, and we immediately communicated out findings to NASA-Ames.

The other part of the transducer evaluation task was to duplicate the current array configuration but supposedly incorporate the latest transducer chip fabrication and circuit-matching techniques. This was done by taking new transducer material, and slicing, coating, and grinding to make the two chips, attaching gold foil leads, mounting in an array holder identical to that of the test-specimen arrays, and then adding the appropriate electrical tuning coils to match the unit to a particular impedance over the operating frequency. Otherwise the sensor was mechanically identical to the original units and in fact utilized the cables from the one that had been dissected. One of the new features added was a special material coating placed on the outer surface of the two chips. This was done as a means of broadbanding the device and also to increase the overall efficiency. The gold foil leads were used to provide a lower-inductance connection to the two surfaces of the chip and also distribute the current more evenly. The impedance of the chip/lead unit was then measured over the frequency band of interest and a tuning inductance of

the appropriate value was calculated. With the chips mounted in the array holder, the tuning coils and feed cables were then attached and the entire unit hermetically sealed. Final testing of overall frequency response and terminal impedance was then done using the techniques outlined previously.

Figure 16 presents the results of the fabrication, showing the efficiency of each chip as a function of frequency. These data include corrections for impedance mismatch and are to be interpreted as one-way energy-conversion efficiency based on a constant-impedance source or load impedance, in this case for 50 ohms. In other words the curves reflect

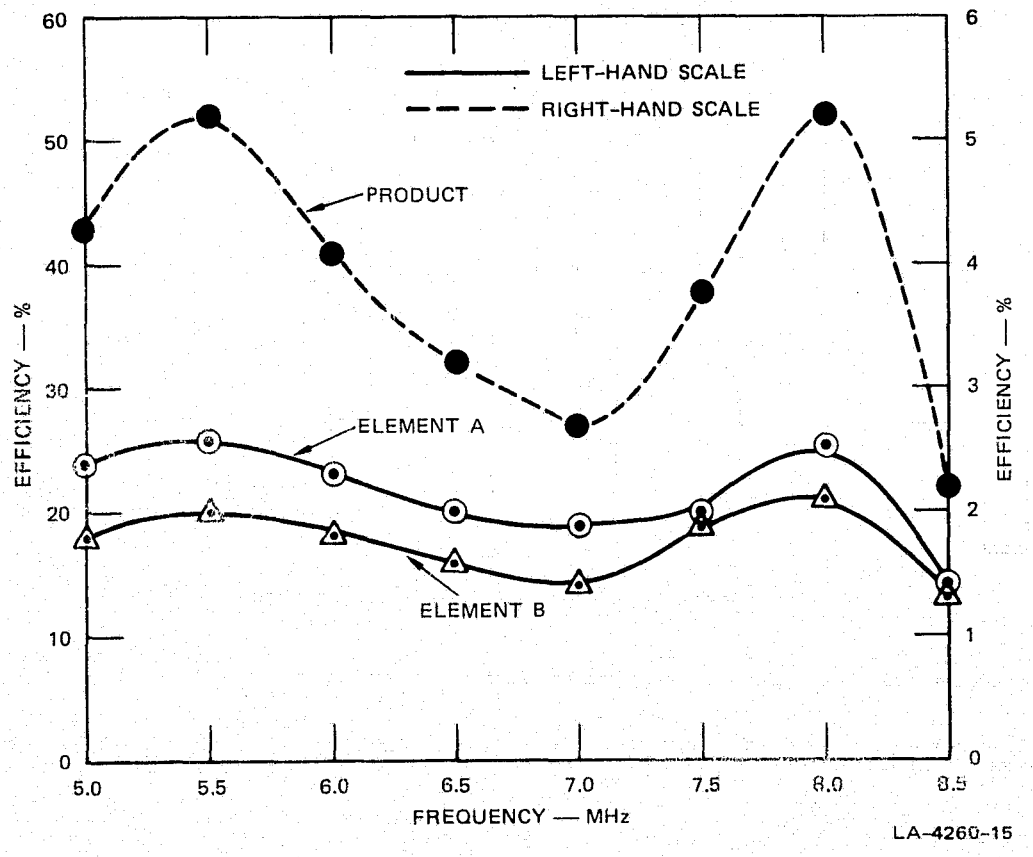

FIGURE 16 EFFICIENCY vs FREQUENCY RESPONSE OF SRI PROTOTYPE TRANSDUCER

actual performance of the sensor array using a constant-impedance generator on one chip and an identical load impedance for the receiver on the other. If different system conditions are used, then the shape and value of the efficiency curve versus frequency can be expected to be different. (See Appendix C for further details concerning transducer characterization and measurement techniques.)

Comparing the SRI sensor with the NASA-Ames model "A" shows that the obvious enhancement has been that of broadbanding, but efficiency has also been improved. This is principally due to the special surface coating and the impedance matching that was used. Thus, not only has the basic transducer efficiency been maintained at a high level, but the bandwidth has been increased by a substantial amount. Alternatively, if the broadband characteristic is not necessary, the special coating can be deleted, which will result in a narrower operating range but one with substantially higher efficiency. In the first case, a given transducer array can be used at any frequency over a large range, which may be advantageous from an experimental point of view. Similarly, that same transducer may be used with a wideband signal such as is necessary for ranging information. If sensitivity is more important, then the high-efficiency narrow-band version is an appropriate choice. The decision then lies with the user rather than the designer.

Although this particular transducer evaluation has been limited to only the chip performance, much can be done to improve the arraying of such chips for a particular application. The task of providing the optimum transducer, of course, relates to the measurement job. In the case of the CW Doppler flow measurement, the main optimization involves illumination-geometry control for clutter rejection and signal enhancement. There are many ideas for better measurement techniques using both the CW and the pulse-Doppler methods, but all depend upon a good transducer array matched to the anatomical conditions where the flow measure is to occur.

VIII CONCLUSIONS

As outlined in Section II of this report, one of the main objectives of this study was to ascertain the amount of sensitivity enhancement that could be expected and achieved by use of the spectral-analysis technique. The starting point is the well-known fact that spectral-analysis provides effective noise suppression for coherent signals or for quasi-CW band-limited signals. In effect, the transform is an integration over the data-sample-set length so that signal spectral-energy density can be optimally separated from noise. For quasi-CW signals the amount of "processing gain" that can be effectively achieved is directly related to the short-term signal bandwidth or to its long-term "acceleration." Thus, a quasi-CW signal that is wandering within a specified bandwidth B at a maximum rate of S Hz/s could be extracted from wideband background noise with an enhancement ratio of about $\sqrt{S}/B$. In the case of blood flow in an artery, the velocity might typically rise from near zero to about 4 kHz equivalent Doppler shift in something less than 50 ms. This represents an acceleration of about 8×10^4 Hz/s, which corresponds to a matched bandwidth of about 300 Hz. If the flowmeter observational bandwidth were 10 kHz, there is the potential enhancement of SNR by a factor of 35, or about 15 dB.

Unfortunately, the spectrum of the blood-flow Doppler signal is rather broadband and, in fact, for the transducer configuration presently used, the spectra are nearly uniform from zero (actually the flowmeter's lower-frequency cutoff) up to the maximum value for any portion of the pulsatile period. As the blood flow rate increases, so does the total energy of the Doppler signal, which increases the wideband SNR. In other words the unprocessed and the processed SNRs are nearly equivalent at

high blood-flow rates, and only at the low rates is any significant improvement achieved by using the spectral-analysis algorithm. This was demonstrated rather well by the controlled in-vivo tests where the operator carefully degraded the data SNR to the point where the L&M flowmeter could barely process the signal using the zero-crossing-counter circuit. The in-vivo test data were digitized, along with the analog pulsatile waveform, and processed using the FFT and the centroid algorithm. Except for minor differences during low flow rates, the two methods provided nearly equal pulsatile waveforms.

The other objective of this study was to demonstrate the feasibility and advantages of applying modern digital recording and processing techniques to blood-flow-rate estimation. Although this brief study did not include accurate flow measurements under controlled and calibrated conditions (in vitro) for absolute evaluation, we do feel that the in-vivo pulsatile comparison tests are valid and that they satisfy the feasibility demonstration goal. For the application in which real-time digital processing is not required, recording on standard digital tape is quite practical at the data rates at which normal ultrasonic Doppler signals occur. For the case of the directional flowmeter made by L&M Electronics, the sampling rate per channel need be no more than 10 kHz and possibly only 7 kHz, and the ADC quantization need be no more than 8-bit resolution. This translates to a throughput bit rate of less than 160 kbits/s. High-speed 9-track digital tape machines can write at a bit rate up to 2 Mbits/s, while standard units provide at least a 200-kbit/s throughput write rate. Total recording-time duration per standard tape roll depends on the data format and the tape write density, but a typical value would be as much as 20 minutes for the assumed input conditions outlined above.

Processing of the data using the FFT and the first-moment algorithm is relatively straightforward but somewhat time-consuming when used on a

general-purpose computer and called in FORTRAN language. The processing of the data shown earlier from the two-channel audio to the final pulsatile output required about one minute of computer time for each second of raw data. This ratio of about 60:1 is primarily a result of the inefficiency of FORTRAN execution time rather than an intrinsic limitation of the computer. If all programming had been done in machine language, the calculations could have been done much faster but still not in real time. Only by implementing the FFT in a special hard-wired logic processor can this type of calculation be done at the rate required for the blood-flow application.

Doing the entire digital processing in real time is just now becoming feasible. Currently available microprocessors and related microcircuitry have the necessary speed and memory size to allow all of the above mentioned mathematical operations to be done as the data are collected. The FFT basic transform operation can be implemented in hardware so that total transform time for a moderate-size time data set (such as 512 points) is less than a few milliseconds. A microprocessor memory cycle time of less than 100 ns and complete instruction times of about 1 μs make the rest of the algorithm calculations rather simple and very fast. The FFT, the first-moment estimate, and the output-data smoothing can easily be done in less than 10 ms.

The other main effort on this contract was an evaluation of the currently in-use CW Doppler flowmeter equipment. This task was completed on the Model 1012 flowmeter manufactured by L&M Electronics. With the improvements that have been made at the suggestion of SRI, this flowmeter now represents the state of the industry for all-solid-state analog processing equipment. This performance is close enough to the physically realizable limits to be used as a standard of comparison.

The ultrasonic transducers that are being used today at NASA-Ames have been investigated and found to be lacking in certain performance parameters. There are fabrication techniques that allow for both better energy efficiency and wider bandwidths. Good quality-control methods will assure a consistent production yield of transducer-array sensors of the desired performance. These techniques are available at SRI as an established group in the Ultrasonics Laboratory.

With the techniques we have provided, NASA can now improve their fabrication techniques so as to obtain better quality control and more consistent results.

Appendix A

EVALUATION OF L&M DOPPLER FLOWMETER MODEL 1012

Appendix A

EVALUATION OF L&M DOPPLER FLOWMETER MODEL 1012

The evaluation of the L&M flowmeter, Model 1012, was performed in two steps. First, the unit's characteristics were measured in considerable detail, exactly as it was configured at the start of the project in May of 1975. Table A-1 summarizes the results of those measurements.

Table A-1

SUMMARY OF SRI MEASUREMENT RESULTS FOR L&M DOPPLER FLOWMETER

Audio bandwidth	10 kHz (folded)
Noise figure	8 dB folded spectrum
Total gain	109 dB to comparators
Desensitization	3 dB for a -50 dBm direct signal
RF source power	2 V rms open circuit
Source impedance	5 ohms
RF amplifier input Z	Approximately 100 ohms (from L&M)
I-and-Q phase shift	45° (should be 90°)
I-and-Q amplitude ratio	Less than 5% error
Comparator hysteresis	Approximately 100 mV positive
Minimum usable signal	-110 dBm at 8 kHz Doppler
Transducer isolation in vivo	76 dB for deep type 66 dB for shallow type
Maximum 2-tone dynamic range	65 dB for reliable Doppler estimate--80 dB potential (noise limited)
Abnormal operation	Due to improper I-and-Q phase shift and offset hysteresis of comparators

The findings, conclusions, and recommendations were then communicated to NASA-Ames and to L&M Electronics Inc., with the understanding that if they were appropriate and were deemed worthy, they would be incorporated into the unit. As the second step in the task, the primary characteristics of the modified unit were rechecked at SRI to determine whether the anticipated improvement was actually achieved. Table A-2 presents the results, after modification, as determined by L&M Electronics. Table A-3 is a listing of the check-measurement values as found by SRI.

The above sequence was completed by 6 June 1975.

Table A-2

SUMMARY OF L&M MEASUREMENT RESULTS FOR L&M DOPPLER FLOWMETER

Audio bandwidth	9.17 kHz measured
Noise figure	4 dB folded 50-ohm source
Total gain	112 dB to comparators
Desensitization	3 dB for a -50 dBm direct signal
RF source power	2 V rms open circuit
Source impedance	5 ohms
RF amplifier input Z	60 ohms (measured)
I-and-Q phase shift	90° at 7 MHz ±18°*
I-and-Q amplitude ratio	Less than 1% (adjusted)
Comparator hysteresis	Approximately 100 mV positive
Minimum usable signal	-116 dBm at 8 kHz Doppler
Transducer isolation in vivo	Not measured
Maximum 2-tone dynamic range	Not measured
Abnormal operation	Not noticeable†

*Fixed by circuit changes suggested by SRI.

†Fixed by adding another D flip-flop for the I-and-Q.

Table A-3

SUMMARY OF POSTFIX REEVALUATION OF L&M DOPPLER FLOWMETER

(a) Relative Phase Shift Between the I-and-Q Channels, P_{in} = -72 dBm

Frequency (MHz)	Phase Shift (degrees)	
	At 8 kHz	At 1 kHz
5.0	67	74
6.0	78	86
7.0	88	94
8.0	96	103
8.8	100	108

(b) RF Receiver CW Sensitivity and Noise Figure

Frequency (MHz)	Noise Power, P_n (dBm)	Noise Figure, NF (dB)
5.0	-125	6
6.0 through 8.8	-127	4

(c) Minimum Usable Signal (Defined for 90% Pulsatile Output) at 8.0 MHz

Audio Frequency (kHz)	Signal Level (dBm)
1.0	-116
2.0	-116
4.0	-117
8.0	-116

(d) Abnormal Operation (None)

Basically the L&M flowmeter performs as advertised. Circuit design and physical layout and construction appears to be good. There are three areas where improvements are possible.

By reference to Figure A-1, the dynamic-range diagram, the relative performance of the cascaded elements of the system can be assessed. The source power amplifier will supply +15 dBm into 50 ohms, but can deliver a maximum of +23 dBm into a 5-ohm load. The waveform is sinusoidal and the amplitude is flat within 1 dB for all of the switch-selectable frequencies.

The receiver portion of the unit has a measured noise figure of 8 dB referenced to the folded 20-kHz audio bandwidth. The actual SSB spot noise figure is 5 dB. The maximum input signal that can be handled by the system through the demodulator is about -42 dBm where substantial departure from linear operation is measurable (3 dB compression). The level at which significant desensitization of small signals occurs is about -50 dBm. Thus, the useful two-tone dynamic range is approximately 76 dB, based on the folded-spectrum noise floor up to the 3-dB desensitization level. The gain of the entire linear system up to the Doppler processor is about 109 dB, so that the rms noise at the comparator is about 25 mV.

The Doppler-processor section of the unit is basically a zero-crossing detector followed by a one-shot and averaging circuit that function as a linear frequency-to-voltage (F/V) converter. The quadrature audio channel is used to sense the Doppler direction and steer the F/V output to either the inverting or noninverting input of the final output buffer amplifier. Thus, the system is bisensitive to Doppler but only when the signals of interest are time-separated in frequency space. The zero-crossing detector is a standard voltage comparator configured to provide a dead-band or hysteresis by use of positive feedback. Since the

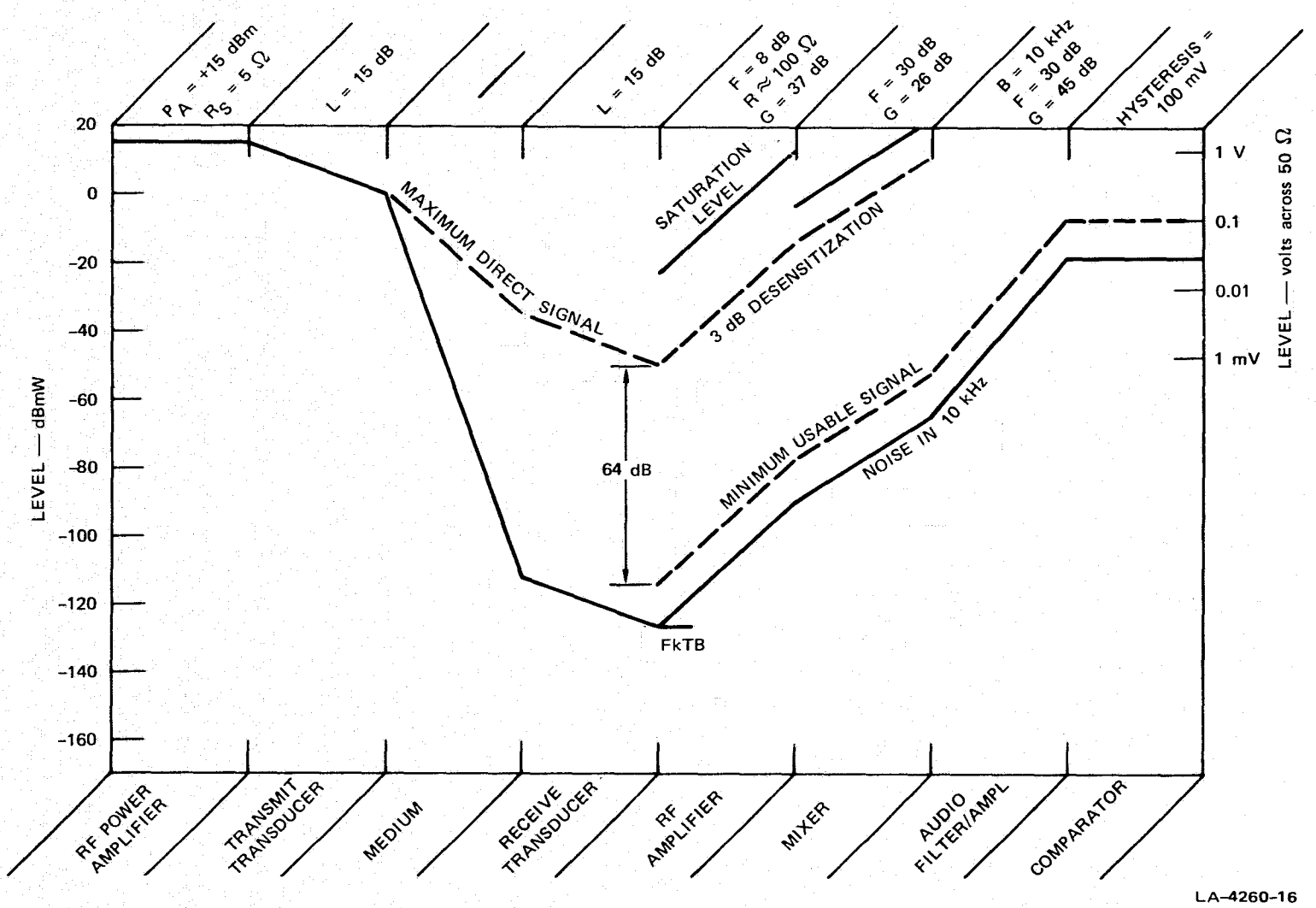

FIGURE A-1 NOISE, GAIN, AND DYNAMIC-RANGE DISTRIBUTION PLOT FOR L&M FLOWMETER

output of the comparator is unipolar, the feedback results in an offset hysteresis band from zero volts up to about 100 mV. Thus, the system noise at 25 mV rms does not cause the comparator to operate until a signal is present that exceeds about -110 dBm at the input, which corresponds to a minimum SNR of about 16 dB.

The quadrature channel has an identical comparator circuit that generates a time-displaced zero-crossing logic signal that is used to determine the Doppler sense. If the Q signal leads by 90°, the opposite occurs. The determination is done in a standard D-type of flip-flop and therefore is absolutely time-dependent.

Measurements of the I-and-Q phase-shift problem appears to stem from the fact that the circuit is composed of a simple R-C high-pass section in the reference and signal paths to the demodulators. The circuit analysis indicates that the capacitor value is incorrect at its current value of 39 pF and should be reduced to about 20 pF. There is a trade-off in that the unit must operate from 5 MHz to 8.4 MHz, which means that this simple R-C phase-shift circuit will provide a 90° shift only at one frequency and will be in error at other frequencies up to ±20°. If the unit must operate over this large a frequency range, and the I-and-Q phase shift must be within a better tolerance than ±20°, then a different design is required such as the compensated wideband quadrature phase shifters. These units are available commercially but can be made up from discrete elements for the specific application.

As mentioned above, the comparators have an offset hysteresis, since the positive feedback comes from the unipolar output. One simple solution would be to counter-offset the positive input by half the amount of the desired hysteresis. Since these values need not be setable, fixed resistors could be inserted to provide the necessary dc offset at either

the positive or the negative inputs. The abnormal Doppler reversal phenomena would be corrected if the above problems were removed.

It should be mentioned that the basic sensitivity of the system is limited to at best a 9-dB SNR for the folded audio spectrum. This result is based on the requirement that an output from the F/V converter is not allowable if no signal is present. Thus, the comparator thresholds must be set to at least the 1% probability level of the random noise amplitude distribution which in this case can be assumed to be Gaussian. The 3-sigma level must then be used, and is the source of the above-mentioned 9 dB. The overall system sensitivity at present seems to be limited to about a 16-dB SNR. Thus the potential improvement to a 9-dB SNR is not very large but is well worth the rather small circuit redesign. Another 3-dB improvement can be gained if the folded audio spectrum could be unfolded and the two Doppler sidebands processed separately in parallel. It is assumed that the desired signals are time-separated in frequency space anyway, but in case they are not, the full coherent method provides that capability also. Finally, if the noise figure of the input RF amplifier could be improved, the ultimate sensitivity of the device would increase by that amount.

In summary, then, about 7 dB improvement could be gained by simply fixing the apparent deficiencies in the present processor, about 2 dB could be gained from an improvement in the RF noise figure, and 3 dB by going to a fully coherent unfolded Doppler processor. This is a potential improvement of 12 dB, or a factor of 4 over the present capability. Of course there is further improvement if spectrum analysis and matched acceleration filtering could be economically incorporated, but that is another problem.

Also, it should be repeated that any improvement in the acoustic transducer efficiency would be a direct improvement in the system performance capability.

Appendix B

EVALUATION OF L&M DOPPLER FLOWMETER MODEL 6010

Appendix B

EVALUATION OF L&M DOPPLER FLOWMETER MODEL 6010

This particular flowmeter is one of the older nondirectional units that includes a telemetry interconnect from the RF head to the Doppler processor chassis. Testing was designed to determine the CW sensitivity over a range of coupled-carrier levels for comparison against the newer directional flowmeter performance. Testing was performed on 11 August 1975 at SRI. Results were verbally transmitted to NASA-Ames and L&M Electronics when personnel from both organizations visited and witnessed the measurement demonstration.

Figure B-1 shows the measurement equipment test setup. A portion of the exciter signal was added to an external signal of adjustable level and frequency so as to simulate the actual flowmeter usage conditions. Operating frequency was that of the flowmeter (8.3 MHz), while the external test signal was set 2 kHz higher in frequency. The processor threshold test control was adjusted for about a 10% reading from noise when only the carrier was applied, and was readjusted for the same conditions as the carrier level was varied. Actual conversion gain was measured using the audio output signal rather than the frequency analog voltage.

Figure B-2 shows the audio output signal level as a function of coupled-carrier level. Above a carrier level of -50 dB relative, the unit ceases to function, presumably due to telemetry saturation. Below that level the effective conversion gain of the detector remains nearly constant until a carrier level of -70 dB is reached. Thereafter the output decreases about 10 dB for each 20-dB reduction of the coupled

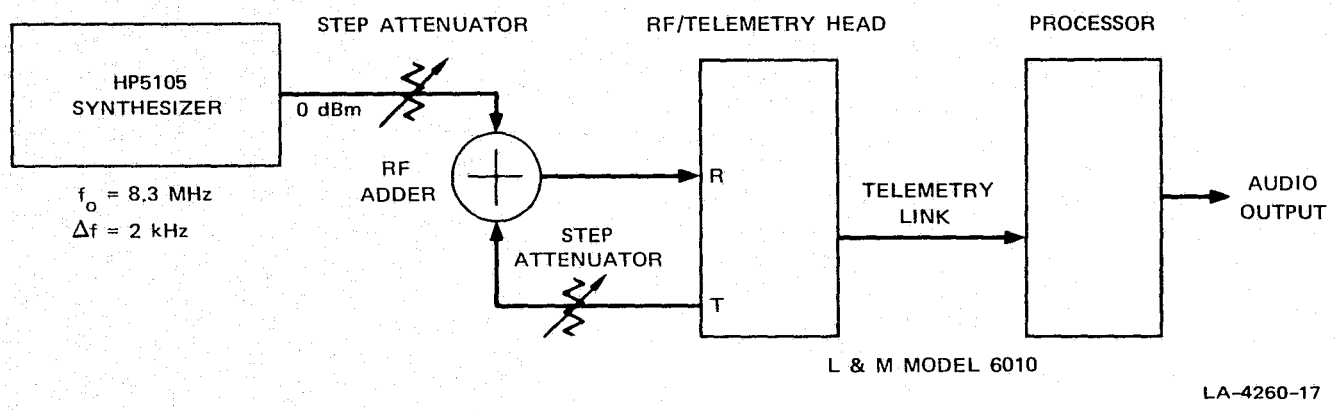

FIGURE B-1 TEST-EQUIPMENT BLOCK DIAGRAM OF NONDIRECTIONAL FLOWMETER

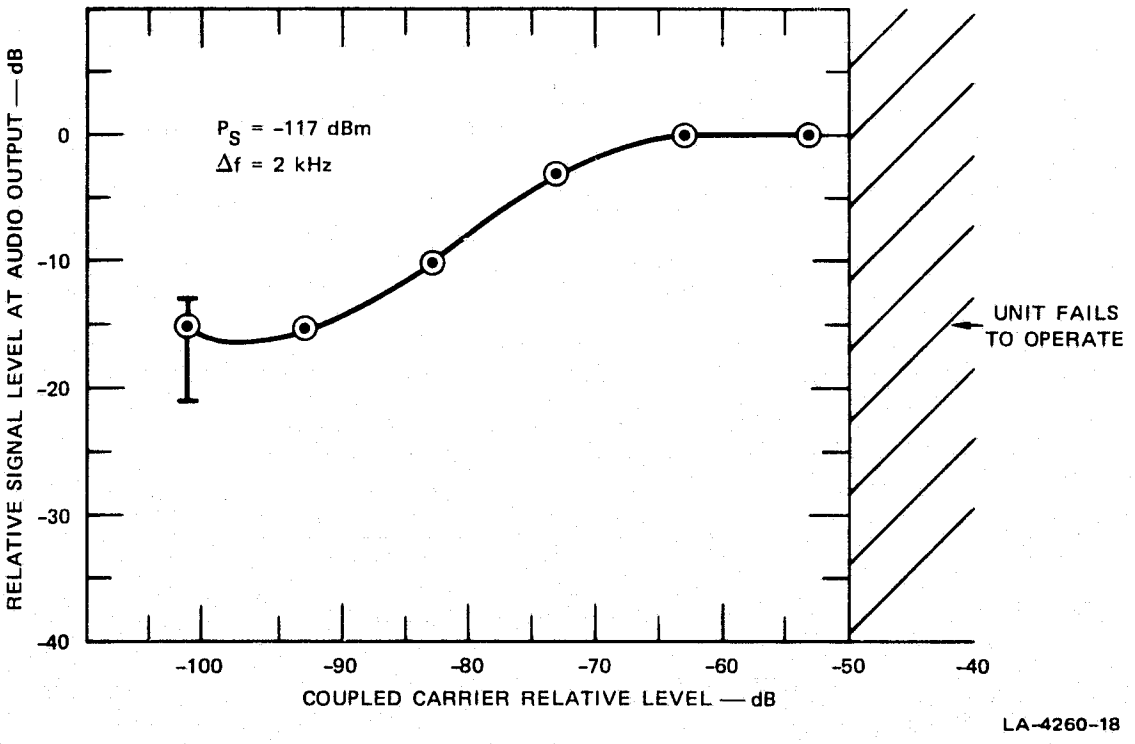

FIGURE B-2 COUPLED-CARRIER EFFECT FOR NONDIRECTIONAL FLOWMETER

carrier until a final level is established, which seems to be a result of carrier leakage within the RF package and not via the external circuitry.

Figure B-3 shows the results for the bandwidth measurement and indicates that the unit has less than a 3-kHz effective bandwidth.

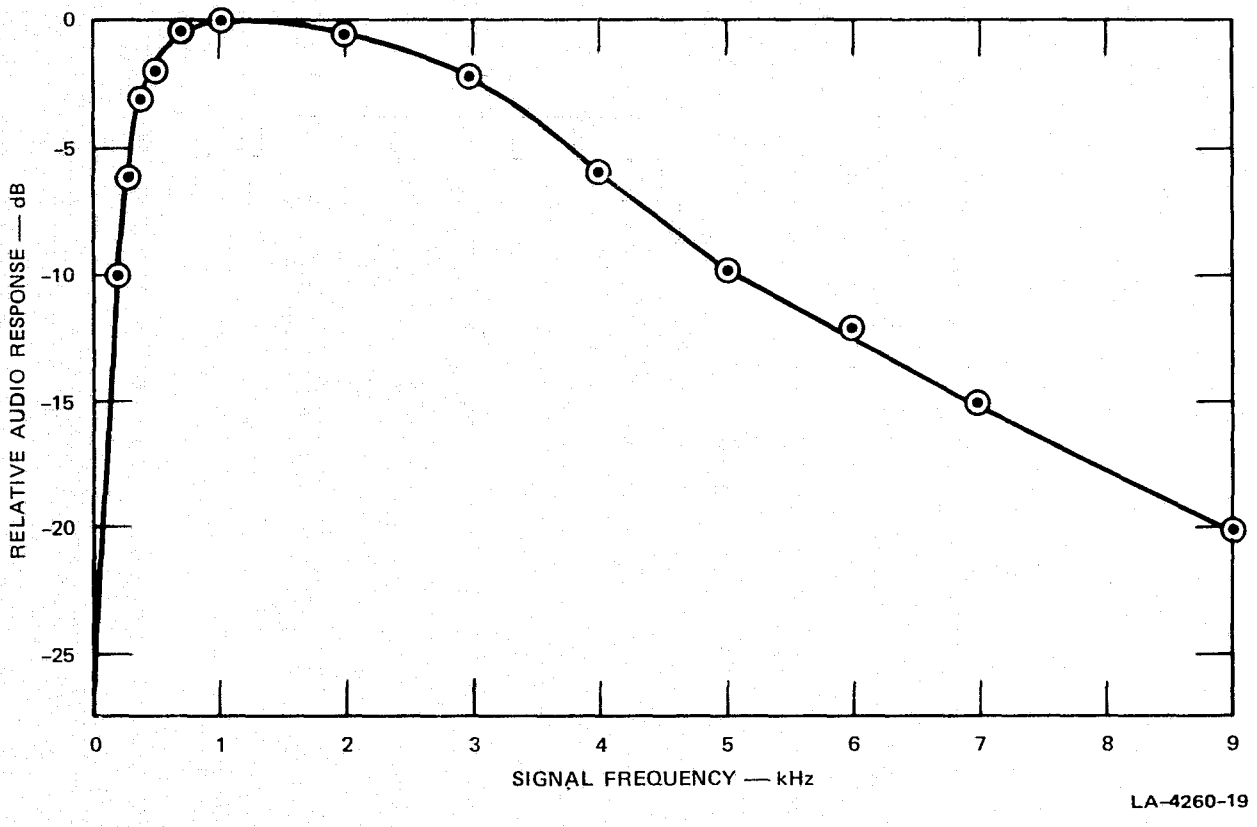

FIGURE B-3 AUDIO BANDPASS FREQUENCY RESPONSE FOR NONDIRECTIONAL FLOWMETER

Appendix C

EVALUATION OF ULTRASONIC-TRANSDUCER EFFICIENCY

Appendix C

EVALUATION OF ULTRASONIC-TRANSDUCER EFFICIENCY

The use of piezoelectric transducers for medical ultrasonic diagnostic testing requires that the element be characterized in a meaningful and consistent manner. The device is an energy converter (electrical acoustic). The conversion efficiency is important because it can be combined with mismatch loss measures to estimate overall subsystem gain and sensitivity. To be consistent with accepted definitions of efficiency, the characterization of the transducer must be done in terms of power delivered and maximum available power output. This makes it absolutely necessary to characterize the device's port impedance carefully.

For applications in which an ultrasonic transducer is used in a bistatic mode (two elements probing, one as a transmitter and the other as a receiver) the overall sensitivity and frequency response can be calculated if the conversion efficiency and terminal impedance of each individual device are known. Mismatch loss from the source and load can be included as well as system element noise contributions. Each element of the system must be characterized fully if any optimization is to be performed.

A simple method of testing an ultrasonic transducer element has been developed and implemented. Figure C-1 outlines the equipment setup; one can see that the test is really a monostatic quasi-CW sonar test in which the target is a large, flat reflecting surface. Testing is performed in an appropriate medium such as water, with the element target placed well within the near-field radiation zone so that distance-dependent correction is not required. The element is excited by a constant-voltage source

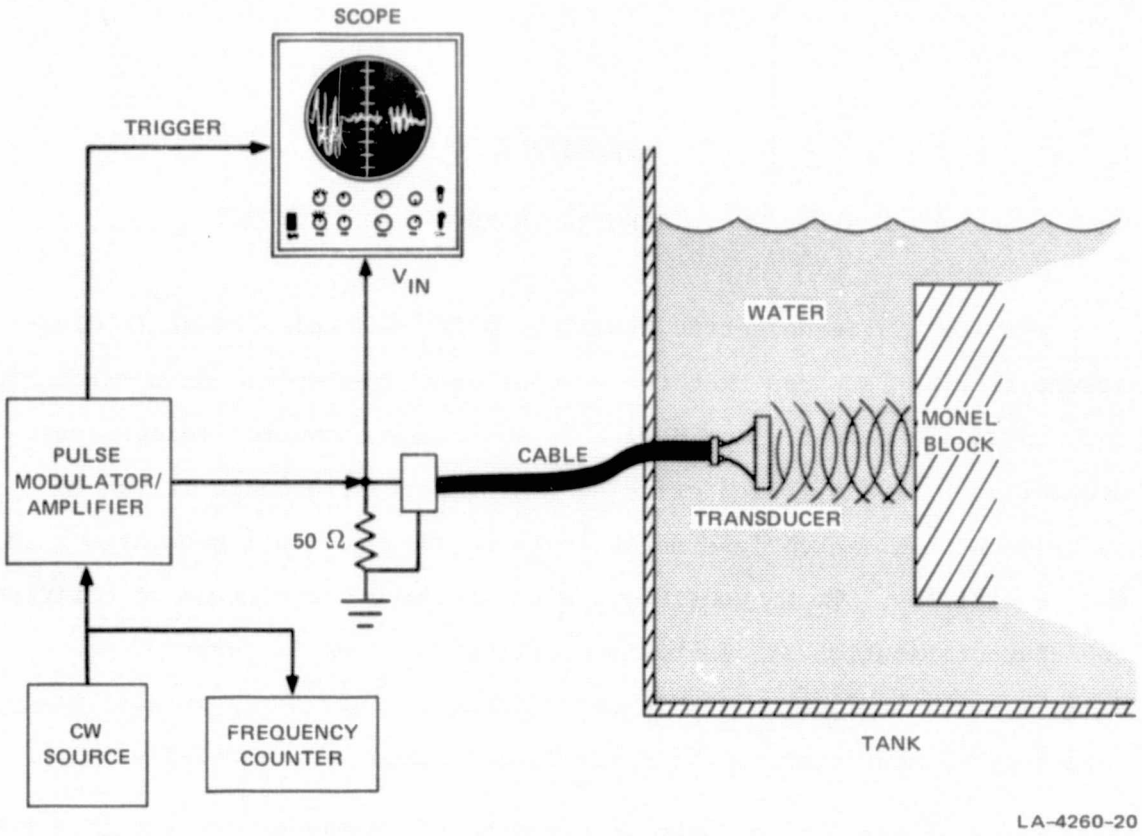

FIGURE C-1 ULTRASONIC TRANSDUCER TEST SYSTEM

and the return-signal voltage is measured across a constant-load resistance. No impedance matching is incorporated. Testing is performed at enough frequency points so that the frequency dependence is adequately described. Figure C-2 illustrates the response that can be obtained. Note that the result implies that the device is rather narrow band. (This chip was not coated or impedance-matched.) However, an inspection of the terminal impedance suggests otherwise. Figure C-3 is the terminal impedance over the same frequency region as that for the voltage response. Note that the impedance varies more than an order of magnitude over the frequency band, which shows that for a constant-voltage source (zero source impedance) the power mismatch is of a similar amount. Thus, the voltage response measured and shown in Figure C-1 is primarily the mismatch

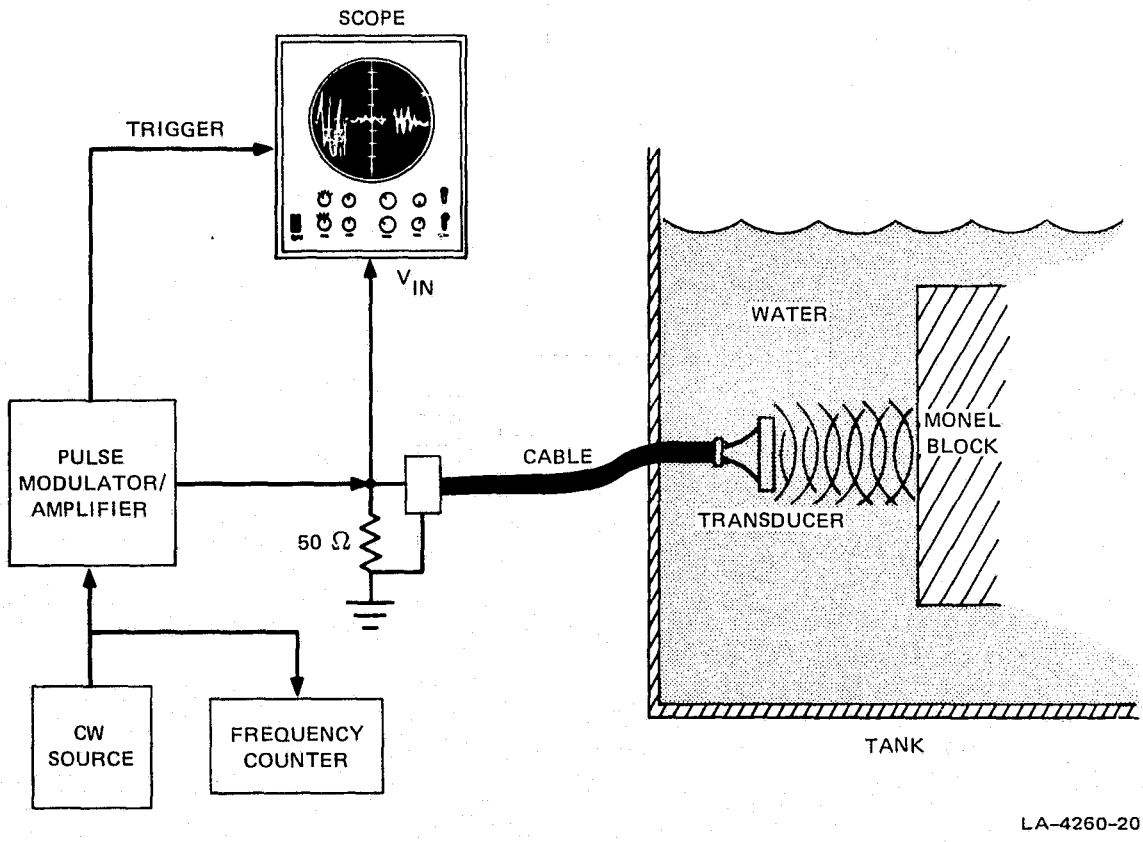

FIGURE C-1 ULTRASONIC TRANSDUCER TEST SYSTEM

and the return-signal voltage is measured across a constant-load resistance. No impedance matching is incorporated. Testing is performed at enough frequency points so that the frequency dependence is adequately described. Figure C-2 illustrates the response that can be obtained. Note that the result implies that the device is rather narrow band. (This chip was not coated or impedance-matched.) However, an inspection of the terminal impedance suggests otherwise. Figure C-3 is the terminal impedance over the same frequency region as that for the voltage response. Note that the impedance varies more than an order of magnitude over the frequency band, which shows that for a constant-voltage source (zero source impedance) the power mismatch is of a similar amount. Thus, the voltage response measured and shown in Figure C-1 is primarily the mismatch

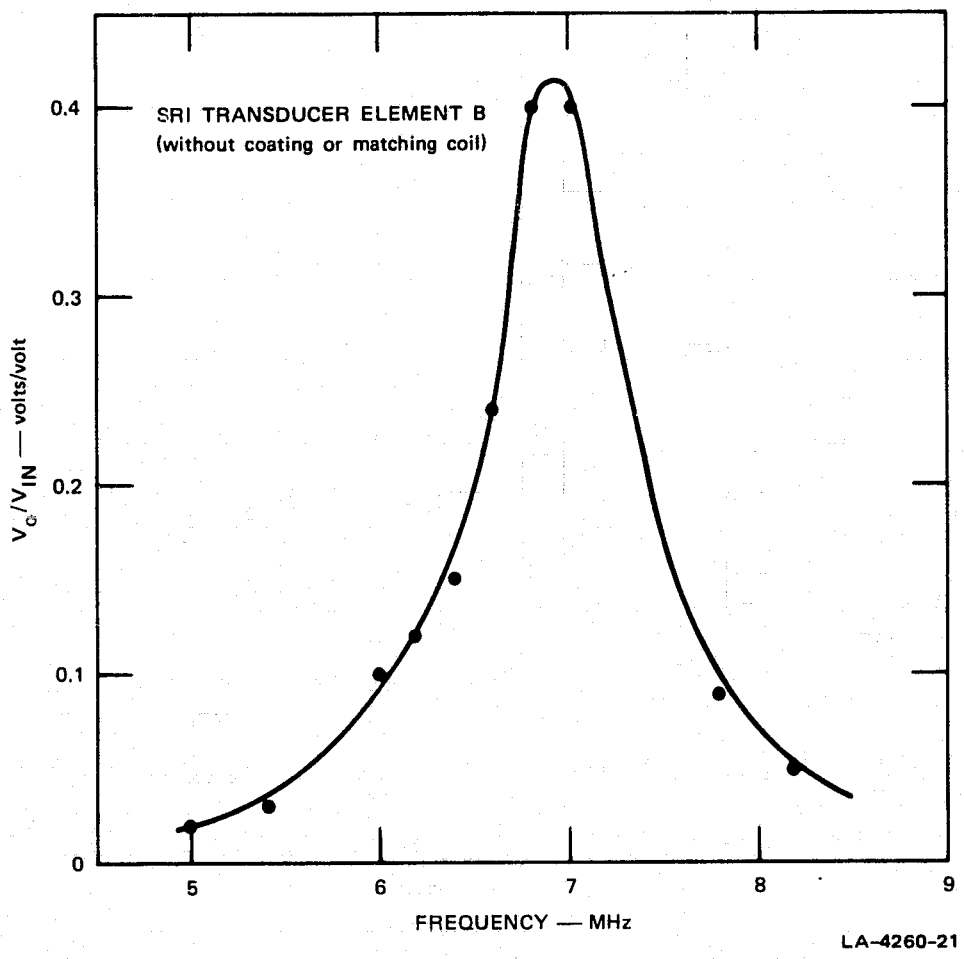

FIGURE C-2 ELEMENT-B TEST RESPONSE, SRI TRANSDUCER

response for the test configuration. When this transducer element is used in a different circuit, the response can and will be considerably different.

Thus we see that the testing of a transducer must include the effects of the test-circuit configuration. It is helpful to consider the problem in terms of, first, the device intrinsic energy-conversion efficiency and, second, the mismatch of imbedding the device in a particular circuit. The impedance-mismatch portion is simply a function of the source and load impedances. From elemental circuit theory the mismatch loss is:

$$M = \frac{4\Re\left(Z_s\right)\Re\left(Z_L\right)}{\left|Z_s + Z_L\right|^2} \qquad \text{(C-1)}$$

where Z_s is the complex series impedance of the source, and Z_L is that for the load. If $Z_s = Z_L^*$ (conjugate match), the mismatch is unity and the response is that due to the device intrinsic conversion loss only.

Applying this relationship to the case where the transducer was tested under constant-voltage excitation and constant resistive load, we

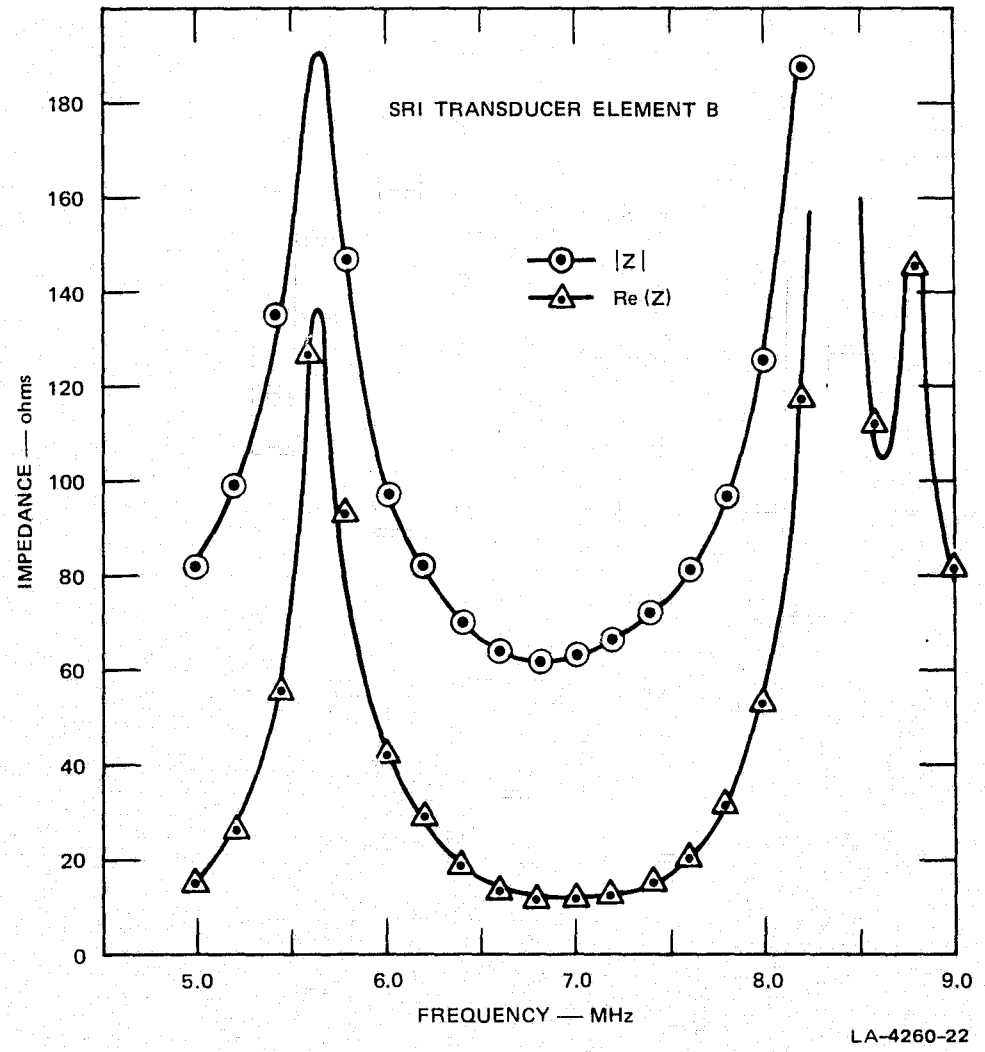

FIGURE C-3 ELEMENT-B TERMINAL IMPEDANCE, SRI TRANSDUCER

can extract the actual conversion efficiency. Here the measurement parameters are input voltage (V_i), output voltage (V_o), device terminal impedance Z (=R + jX), and load resistance R_L (=50 ohm). The power delivered to the device is:

$$P_i = \left(V_i / |Z|\right)^2 R(Z) \quad . \tag{C-2}$$

The output power is simply

$$P_o = V_o^2/50 \quad . \tag{C-3}$$

Efficiency is defined as the ratio of the maximum available output power to the delivered input power. Thus we have

$$\text{Test Efficiency} = \left(P_o/M\right)/P_i \quad . \tag{C-4}$$

Since the test was performed in a reflection mode, the one-way electrical-to-acoustic (or acoustic-to-electrical) energy-conversion efficiency of the device is the square root of the above expression. Therefore

$$\text{Efficiency (device)} = \sqrt{\left(P_o/M\right)/P_i} \quad . \tag{C-5}$$

Applying this to the specific case at hand we obtain

$$E = \frac{V_o}{2\,V_i} \frac{|Z|}{R(Z)} \frac{|50 - Z|}{50} \quad . \tag{C-6}$$

Figure C-4 shows the results of performing these calculations using the data shown in Figures C-2 and C-3. Note that the intrinsic efficiency of the element is different than that indicated by the test in that the device bandwidth is wider and the peak is shifted in frequency.

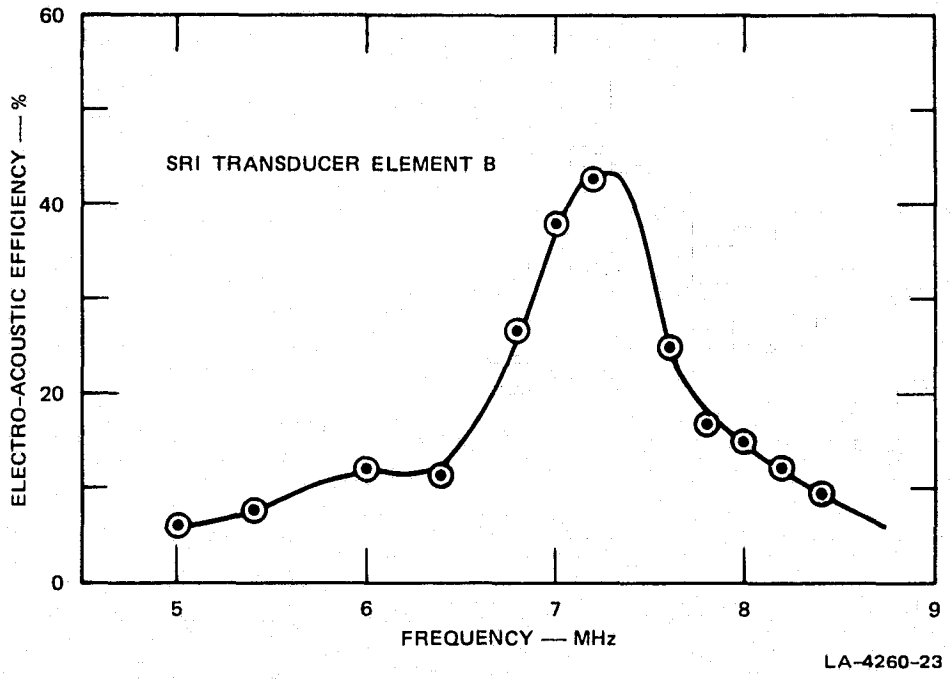

FIGURE C-4 ELEMENT-B INTRINSIC ELECTROACOUSTIC EFFICIENCY, SRI TRANSDUCER

A companion element was tested in the same manner and Figures C-5, C-6, and C-7 summarize those results. Note here that the element had a broader bandwidth and smaller impedance variation than the element in Figure C-4. This can be attributed to the fact that the surface of the element was coated with a special substance and a matching coil added.

The two elements were mounted into a holder along with their associated tuning inductors and feed cables to form a special-purpose transcutaneous ultrasonic Doppler blood-flow sensor. It is instructive to calculate the expected transducer sensor gain as a function of frequency under assumptions of particular drive and load impedance condition, and then compare this with actual in-vivo flow velocity measurements.

A blood-flow test setup was configured to utilize both a 50-ohm signal source to drive one element and a 50-ohm receiver to amplify the signals received on the other element. Figure C-8 shows the equipment setup. Given the condition that both the source and the load impedances

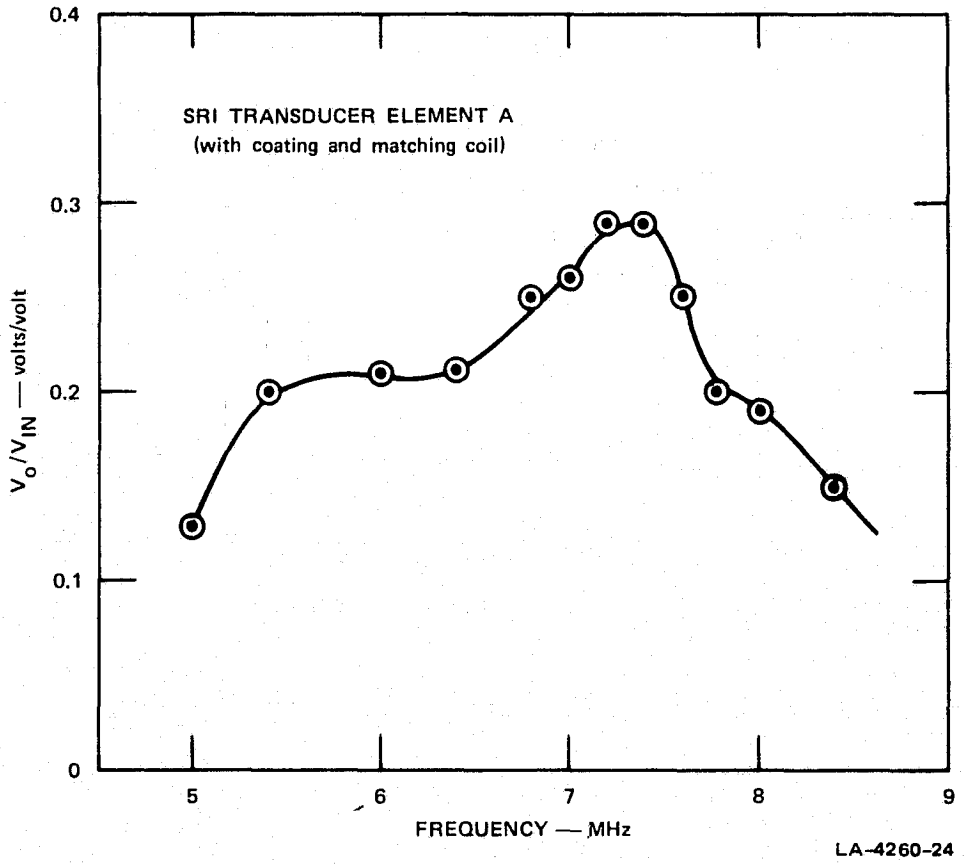

FIGURE C-5 ELEMENT-A TEST RESPONSE, SRI TRANSDUCER

are resistive at 50 ohms, one can calculate the expected sensor frequency response from the element efficiency and terminal impedance values. The overall response equation is:

$$E' = E_a \cdot M_a \cdot E_b \cdot M_b \quad . \tag{C-7}$$

The efficiency values for E_a and E_b are taken from Figures C-4 and C-7 while the mismatch factors M_a and M_b are calculated from use of Eq. (C-1) and the element terminal impedance values shown in Figures C-3 and C-6. Figure C-9 shows the result as calculated over the 5.0-to-8.4-MHz frequency band. Note that when the sensor is used in the bistatic mode (assuming acoustic loss to be constant with frequency) the effective

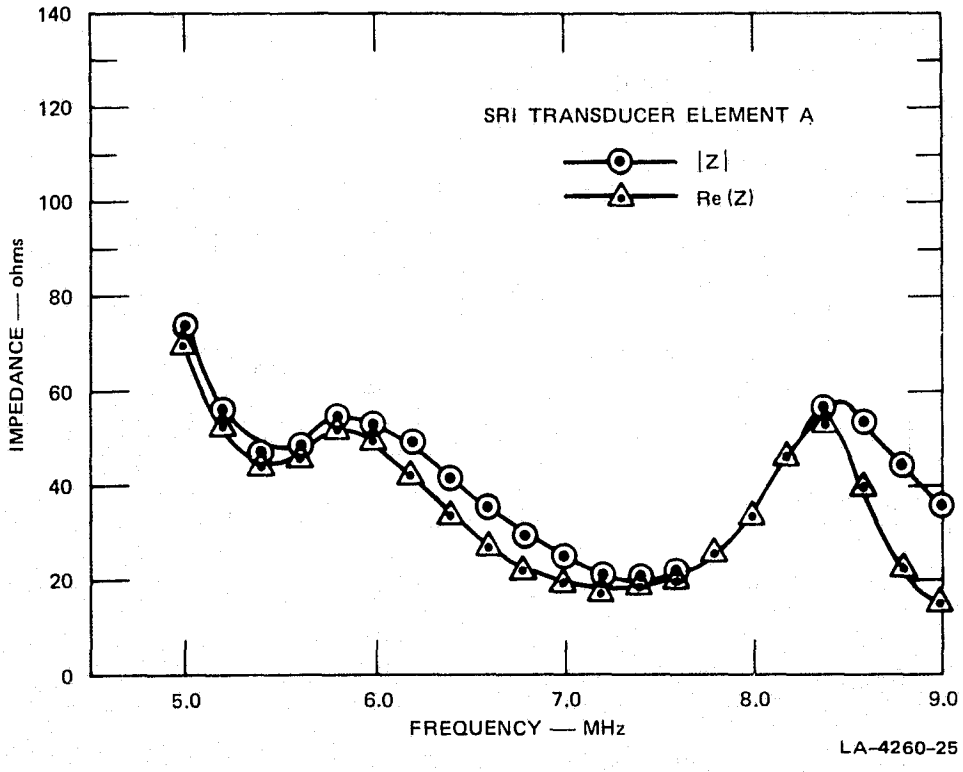

FIGURE C-6 ELEMENT-A TERMINAL IMPEDANCE, SRI TRANSDUCER

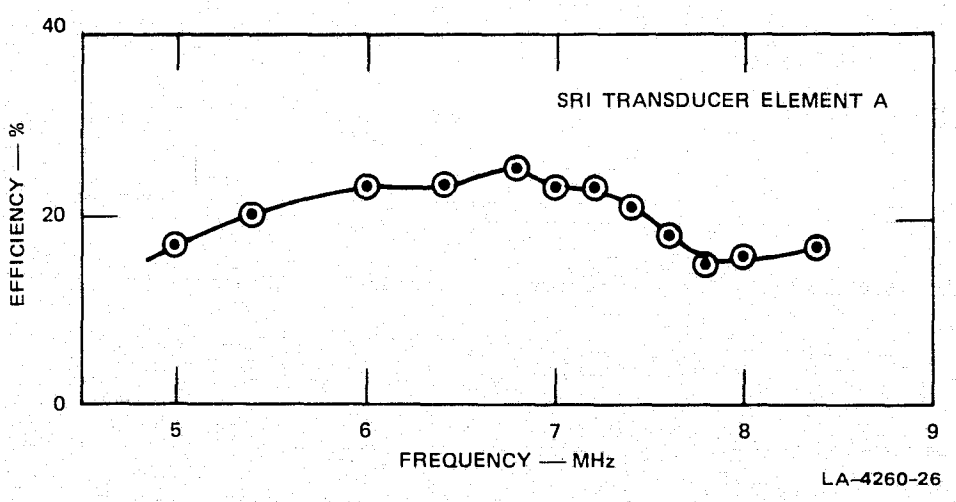

FIGURE C-7 ELEMENT-A INTRINSIC ELECTROACOUSTIC EFFICIENCY, SRI TRANSDUCER

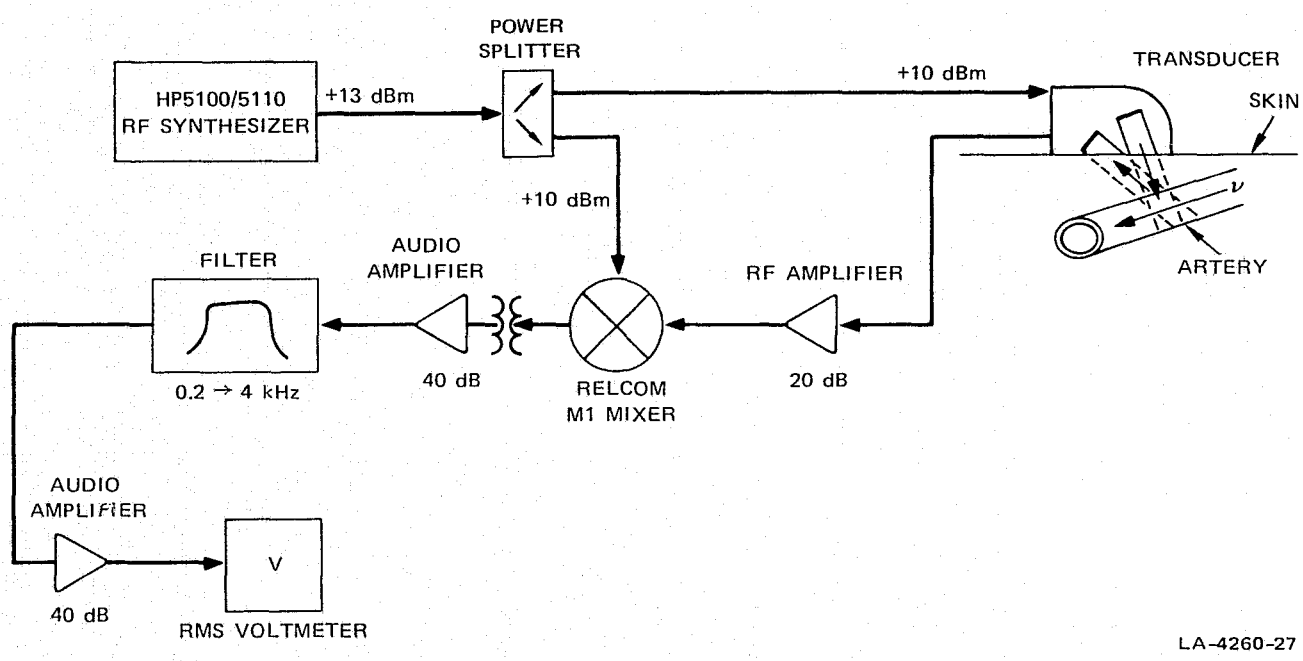

FIGURE C-8 LABORATORY NONDIRECTIONAL DOPPLER BLOOD-FLOWMETER SYSTEM

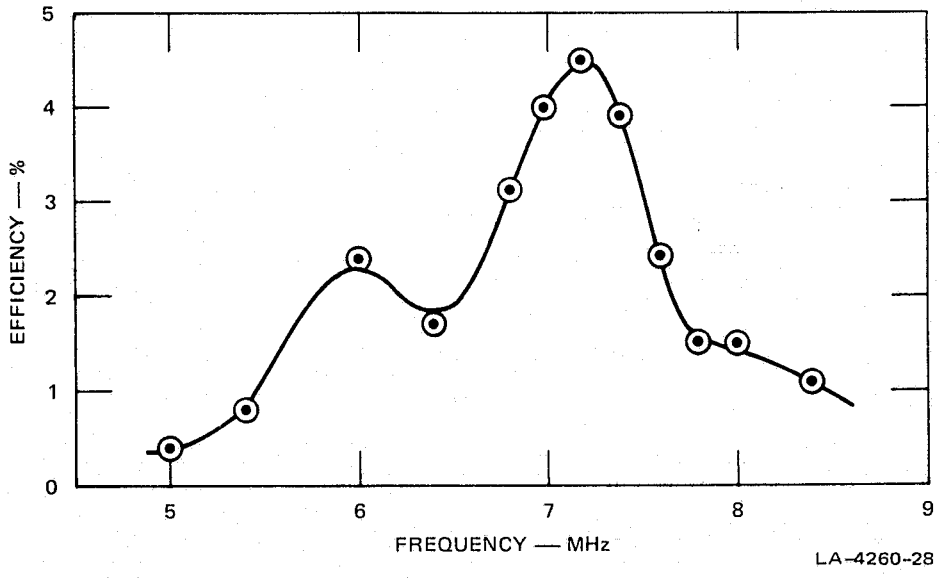

FIGURE C-9 OVERALL EFFICIENCY OF SRI TRANSDUCER ARRAY

amplitude response is very broad in frequency, in sharp contrast with the initial measurements made of the elements. Figure C-10 shows the results obtained when the sensor was used with the Doppler blood-flow equipment under actual in-vivo testing. The agreement between these data and the calculated results shown in Figure C-9 is quite adequate when one includes the facts that neither the source nor the receiver impedance was 50-ohms over the frequency band, and that acoustic propagation loss in tissue and scattering from blood cells are frequency-sensitive to some degree.

The point to keep in mind is that the performance that one should expect from any energy-conversion device will be determined in part by the impedance relationships of the circuit in which it is employed. Simple "convenient" testing methods are preferable, but one must be sure to compensate such data for the more complicated effects of arbitrary circuitry before a performance prediction can be made. Only by this means can modern optimization techniques be employed to assure that a given application will be successful in its implementation.

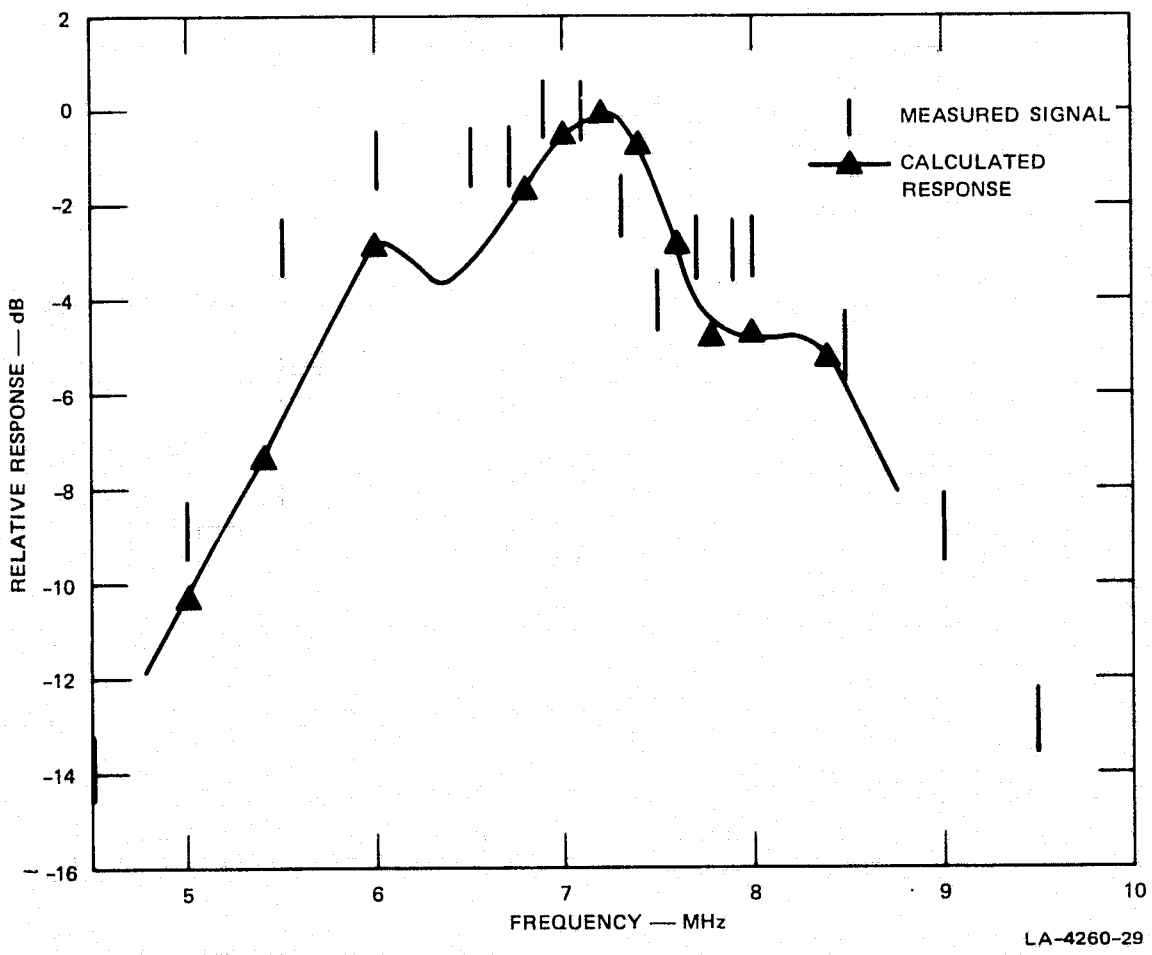

FIGURE C-10 IN-VIVO DOPPLER BLOOD-FLOW DATA FOR SRI TRANSDUCER ARRAY

Another important reason for characterizing the transducer in both efficiency and impedance terms is for optimal matching to obtain best noise figure where low SNRs are expected. It is well documented that for a given amplifier noise figure and input impedance, there is an optimum source impedance that will minimize the overall system noise figure. Even where conditions will not afford much enhancement by this procedure, it still is necessary to know impedances in order to achieve an acceptable level of performance.

Finally, one should always consider the implications of having a less-than-optimum system efficiency or sensitivity. In the case of

medical diagnostics via ultrasonics, it behooves the equipment designer to make sure his system minimizes patient exposure to excessive and possibly harmful radiation. A poorly designed or improperly matched sensor transducer will require that the illumination intensity be higher than is necessary in a more sensitive system, with the attendant higher risk to the patient.

REFERENCES

1. W. R. Brody, Theoretical Analysis of the Ultrasonic Blood Flowmeter, A Dissertation for the Degree of Doctor of Philosophy, Stanford University, Stanford, California (October 1971).

2. M. B. Histand et al., "Development of Ultrasonic Methods for Hemodynamic Measurements," Semi-Annual Progress Report, NASA Grant NSG-2009, Colorado State University, Ft. Collins, Colorado (February 1975).